Synthesis and *Ex Vivo* Biological Evaluation of Gallium-68 Labelled NODAGA Chelates Assessing Cardiac Uptake and Retention

Supporting Information

Bradley E. Osborne,[†,‡] Thomas T. C. Yue,[†] Edward C. T. Waters,[‡] Friedrich Baark,[‡] Richard Southworth,[*,‡] Nicholas J. Long[*,†]

[†]*Department of Chemistry, Imperial College London, Molecular Sciences Research Hub, White City Campus, Wood Lane, London, W12 0BZ, U.K.*

[‡]*Division of Imaging Sciences and Biomedical Imaging, St. Thomas' Hospital, King's College London, London, SE1 7EH, U.K.*

Contents

NMR Spectra

(4-(Aminomethyl)benzyl)triphenylphosphonium bromide (**2a**)

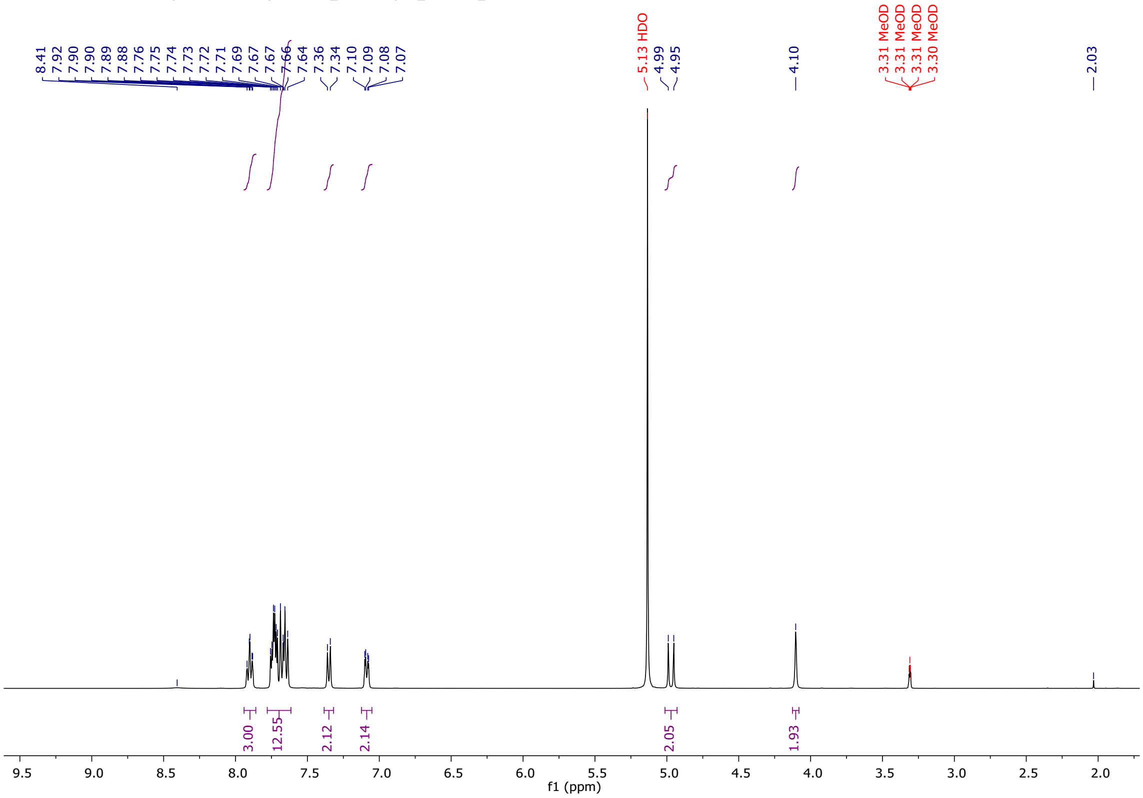

Figure S1: ^{1}H NMR spectrum (MeOD, 400 MHz, 298 K).

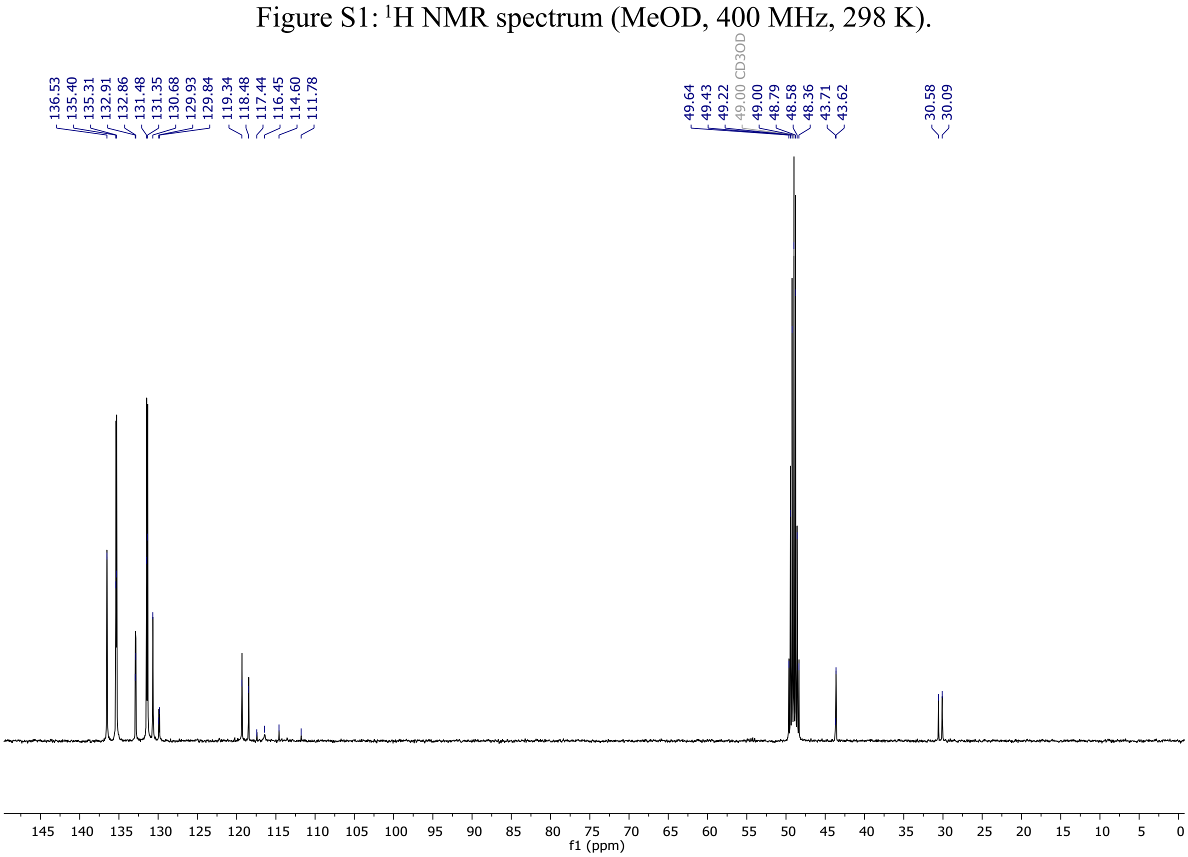

Figure S2: $^{13}C\{^{1}H\}$ NMR spectrum (MeOD, 100 MHz, 298 K).

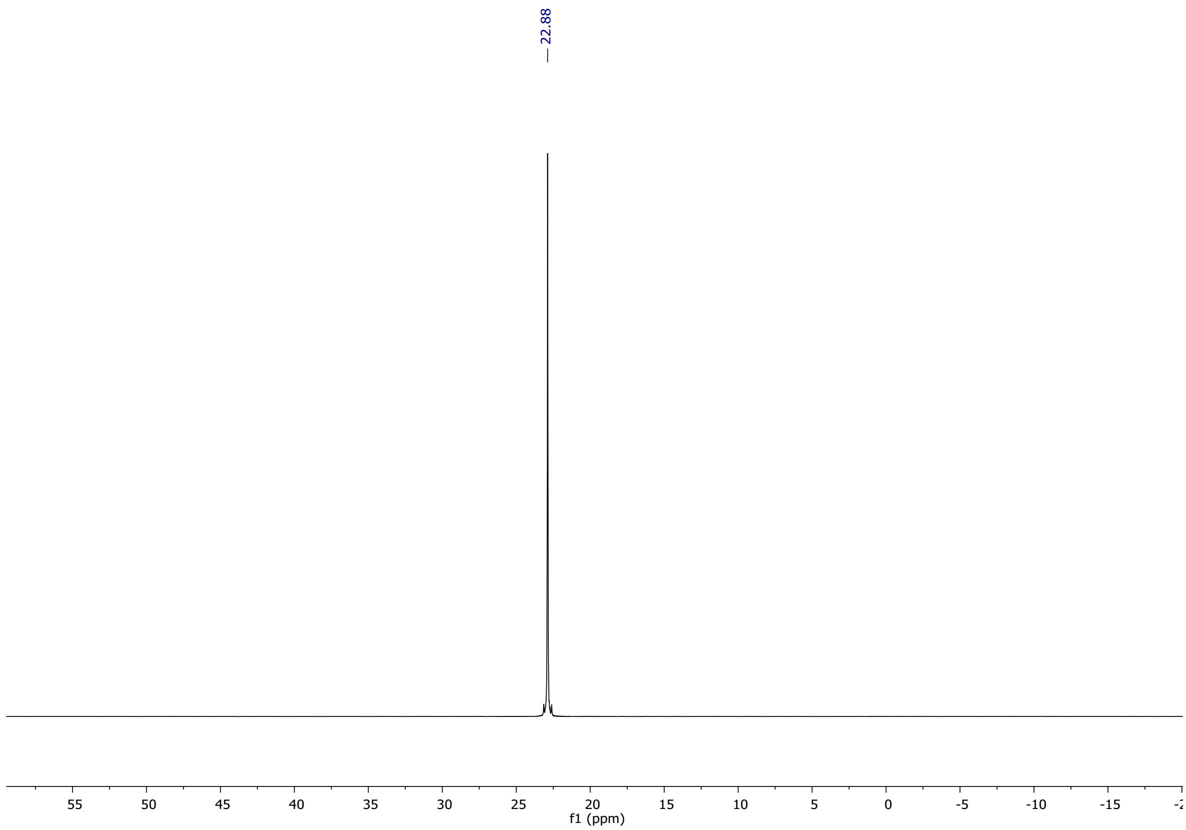

Figure S3: $^{31}P\{^{1}H\}$ NMR spectrum (MeOD, 162 MHz, 298 K).

(4-(Aminomethyl)benzyl)tri(4-methylphenyl)phosphonium bromide (**2b**)

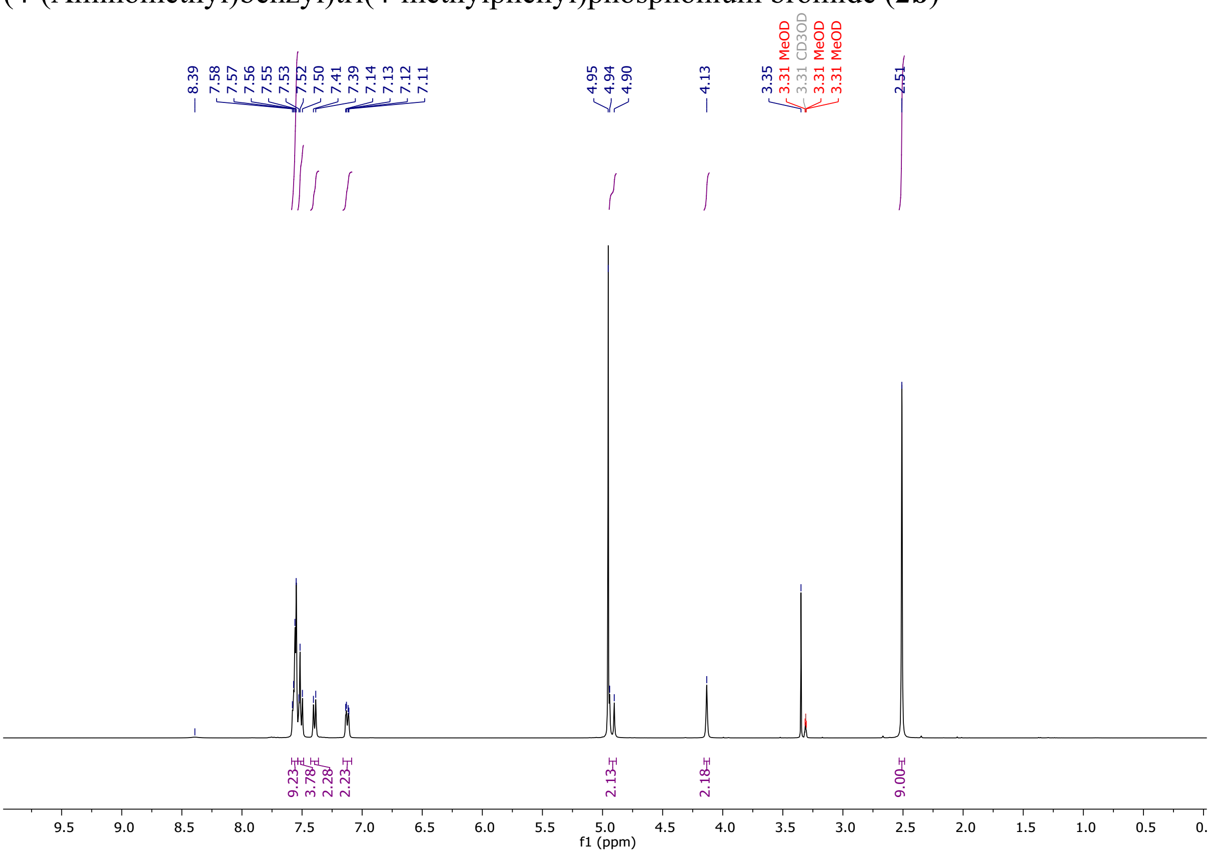

Figure S4: ^{1}H NMR spectrum (MeOD, 400 MHz, 298 K).

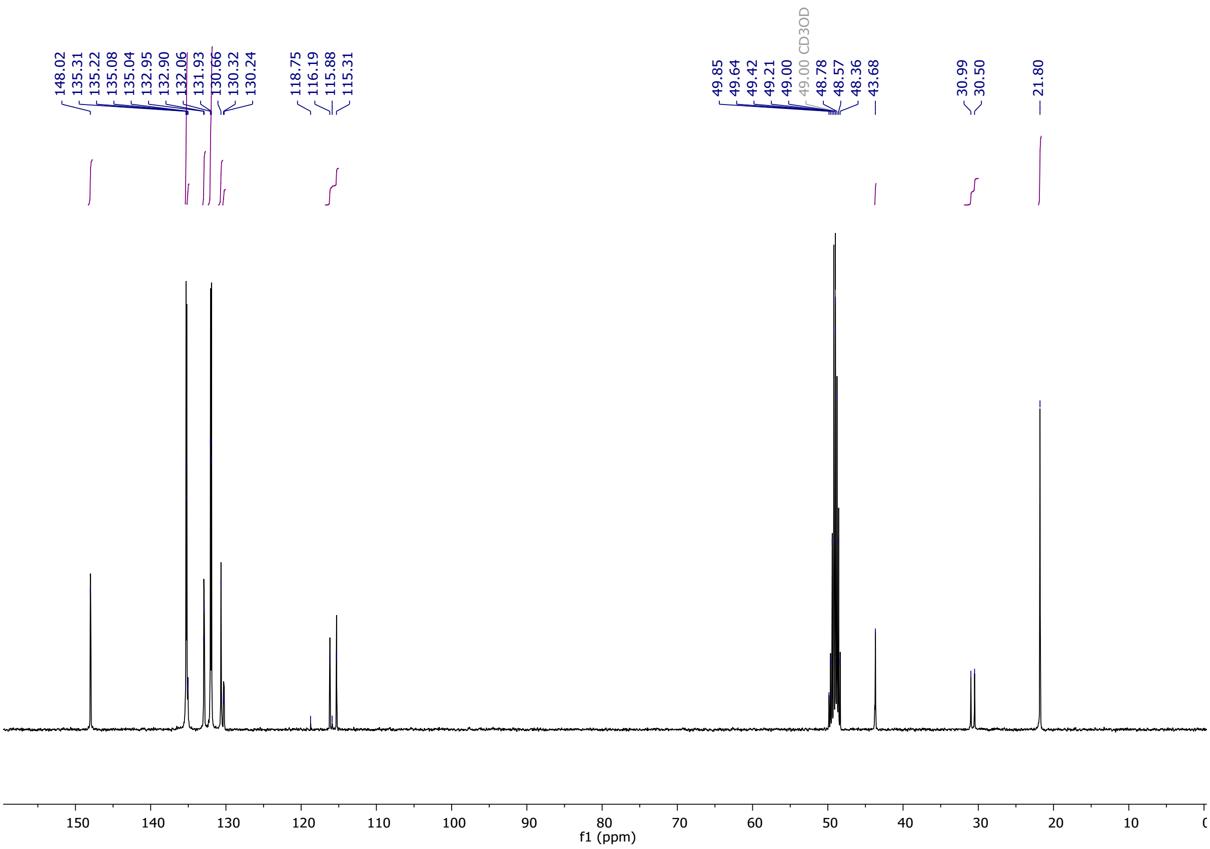

Figure S5: $^{13}C\{^{1}H\}$ NMR spectrum (MeOD, 100 MHz, 298 K).

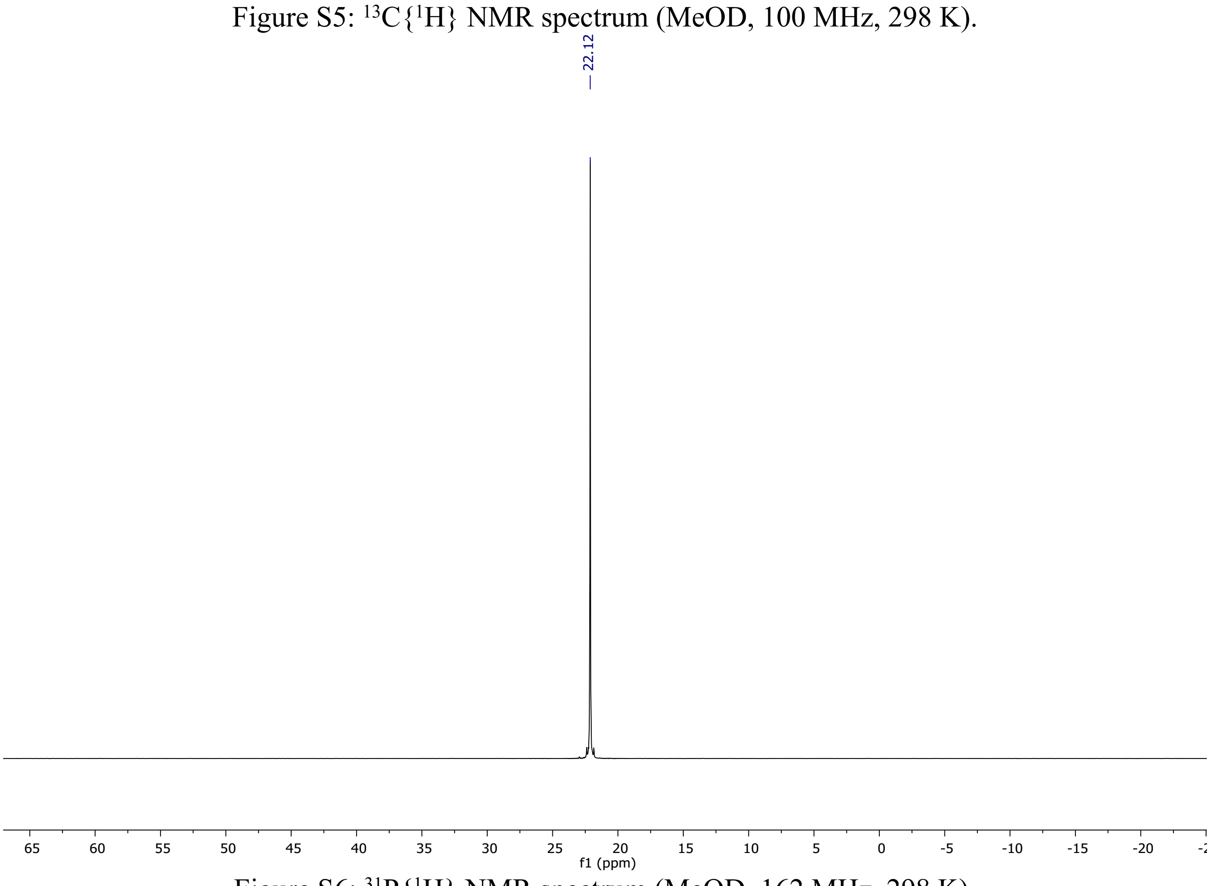

Figure S6: $^{31}P\{^{1}H\}$ NMR spectrum (MeOD, 162 MHz, 298 K).

(4-(Aminomethyl)benzyl)tri(3,5-dimethylphenyl)phosphonium bromide (**2c**)

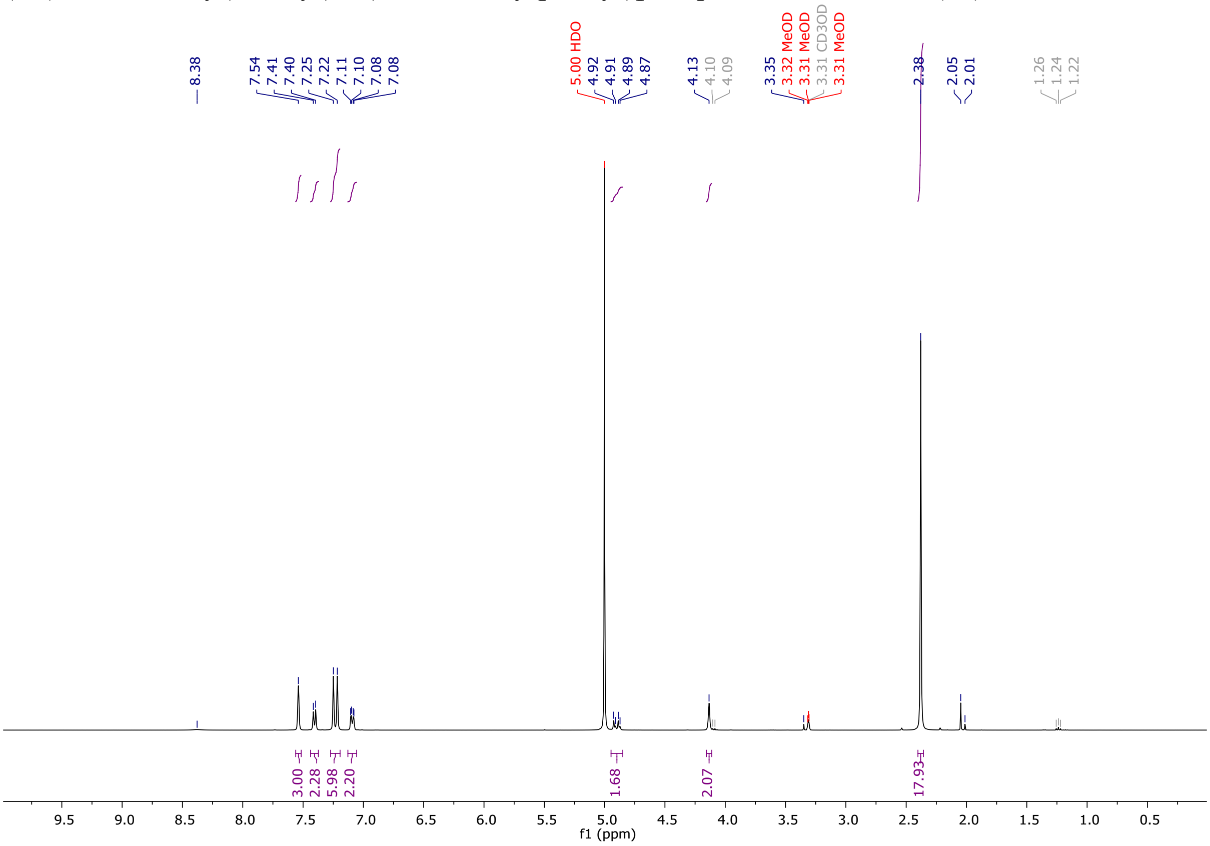

Figure S7: ^{1}H NMR spectrum MeOD, 400 MHz, 298 K).

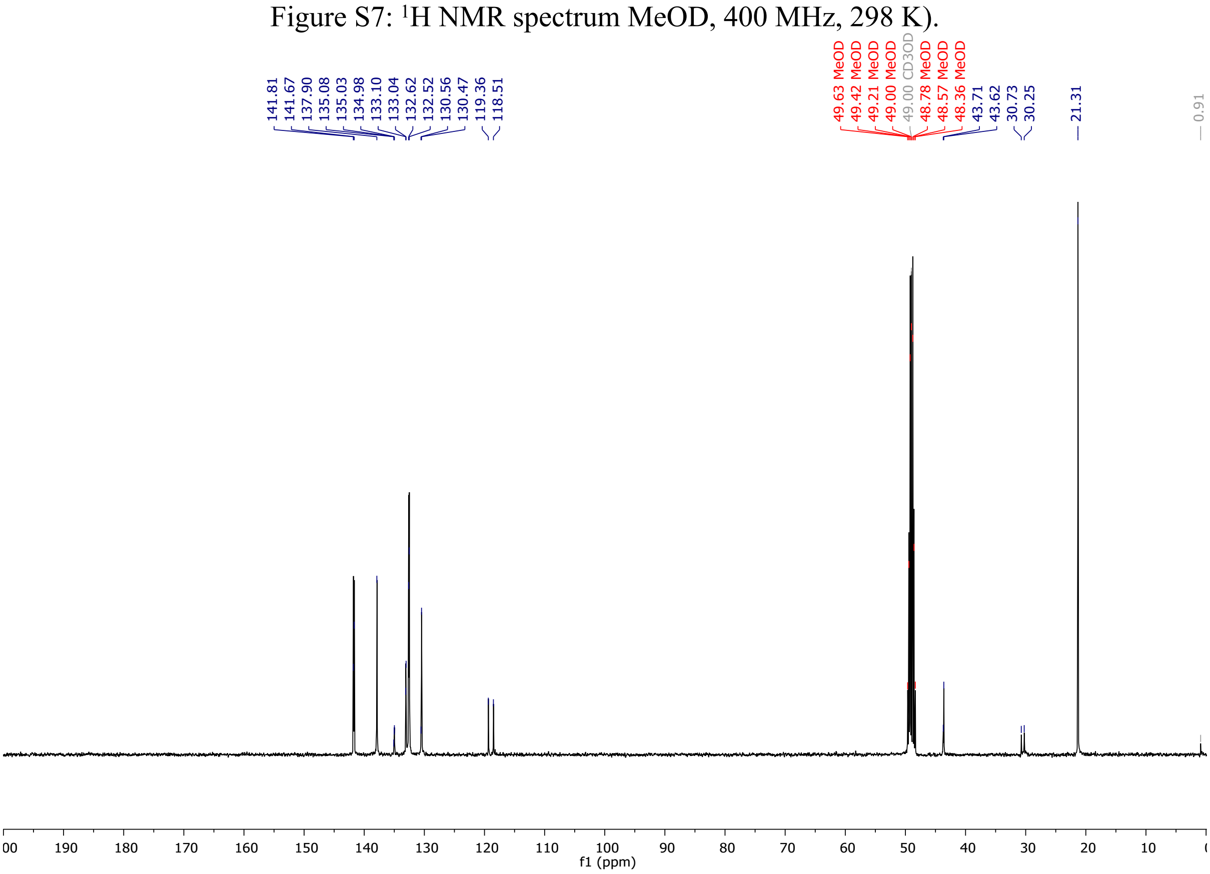

Figure S8: $^{13}C\{^{1}H\}$ NMR spectrum (MeOD, 100 MHz, 298 K).

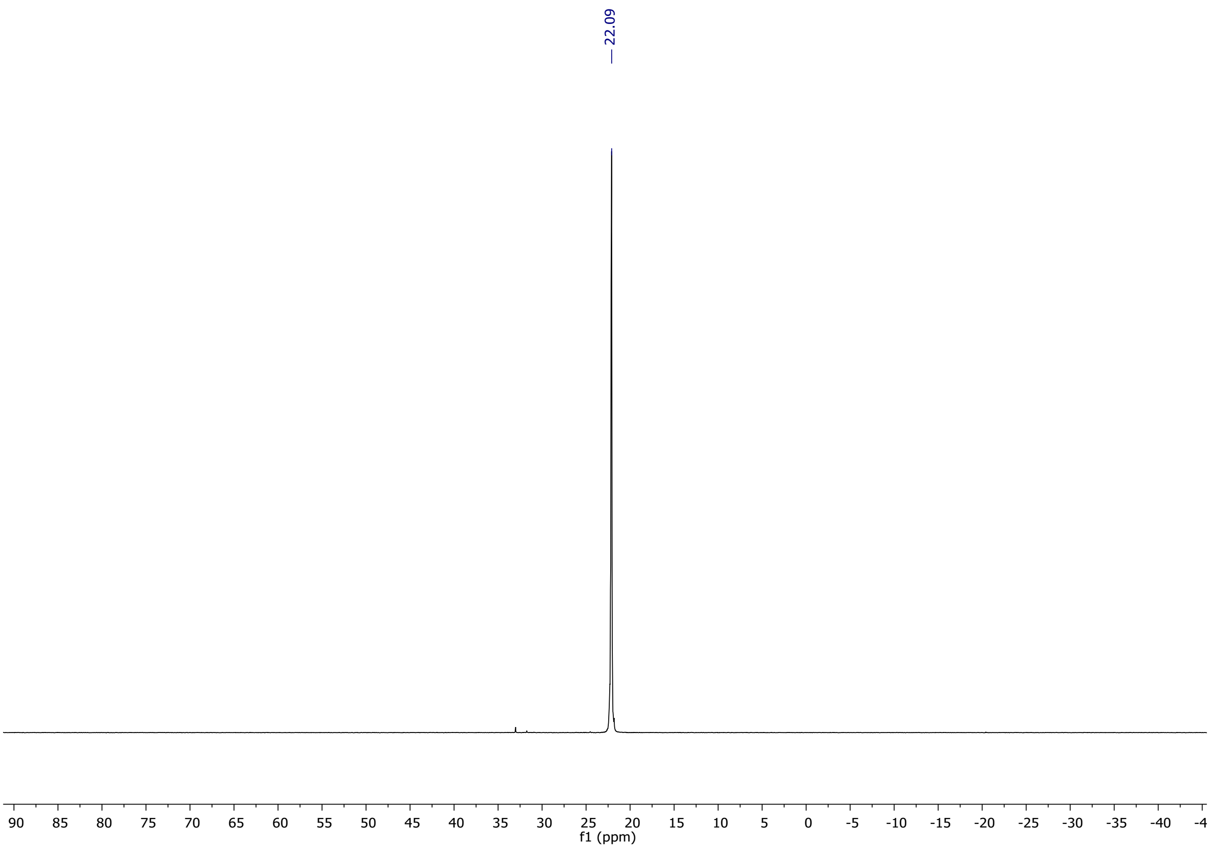

Figure S9: $^{31}P\{^{1}H\}$ NMR spectrum (MeOD, 162 MHz, 298 K).

(4-((4-(4,7-Bis(2-(*tert*-butoxy)-2-oxoethyl)-1,4,7-triazonan-1-yl)-5-(*tert*-butoxy)-5-oxopentanamido)methyl)benzyl)triphenylphosphonium bromide (**3a**)

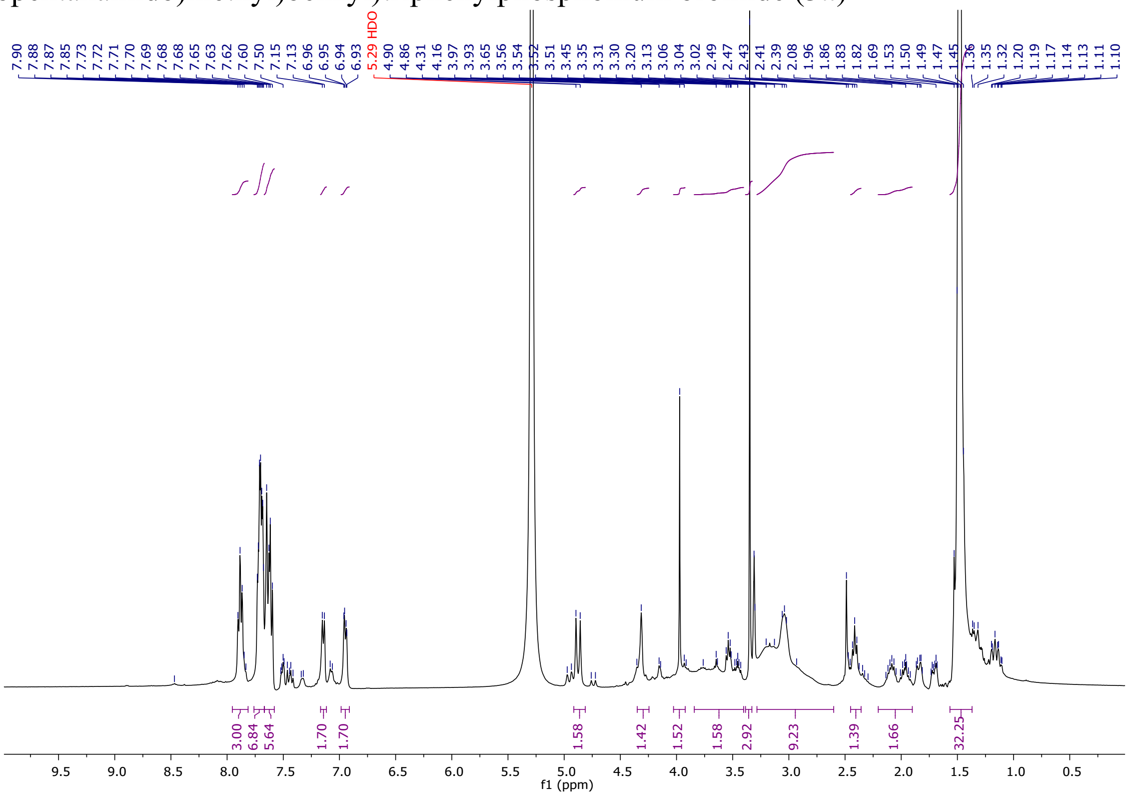

Figure S10: ^{1}H NMR spectrum (MeOD, 400 MHz, 298 K).

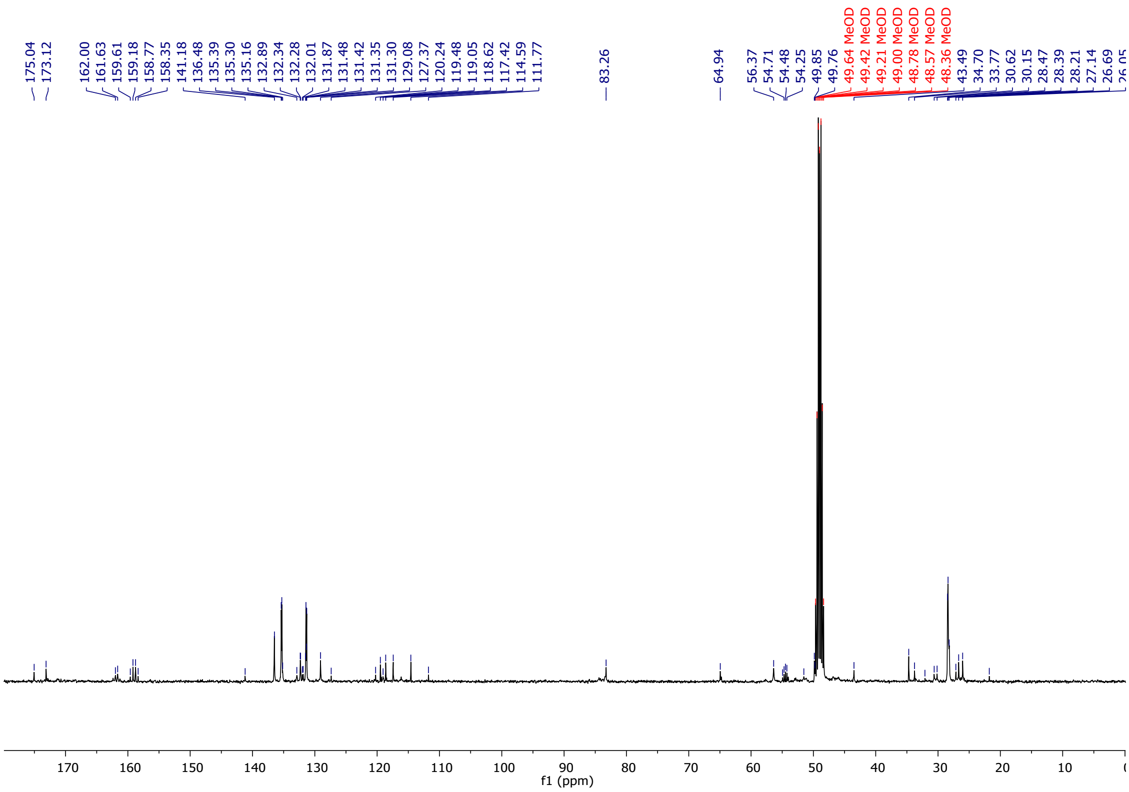

Figure S11: $^{13}C\{^{1}H\}$ NMR spectrum (MeOD, 100 MHz, 298 K).

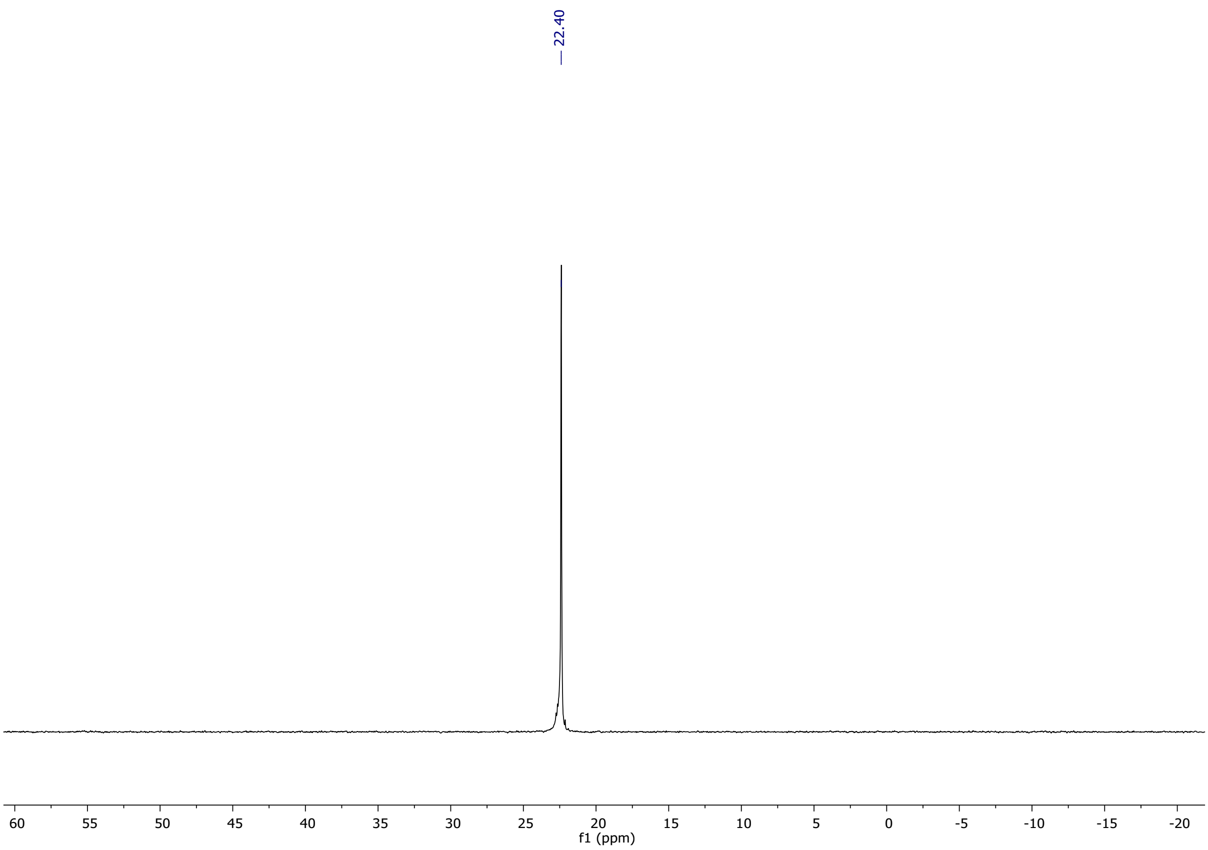

Figure S12: $^{31}P\{^{1}H\}$ NMR spectrum (MeOD, 162 MHz, 298 K).

(4-((4-(4,7-Bis(2-(*tert*-butoxy)-2-oxoethyl)-1,4,7-triazonan-1-yl)-5-(*tert*-butoxy)-5-oxopentanamido)methyl)benzyl)tri(4-methylphenyl)phosphonium bromide (**3b**)

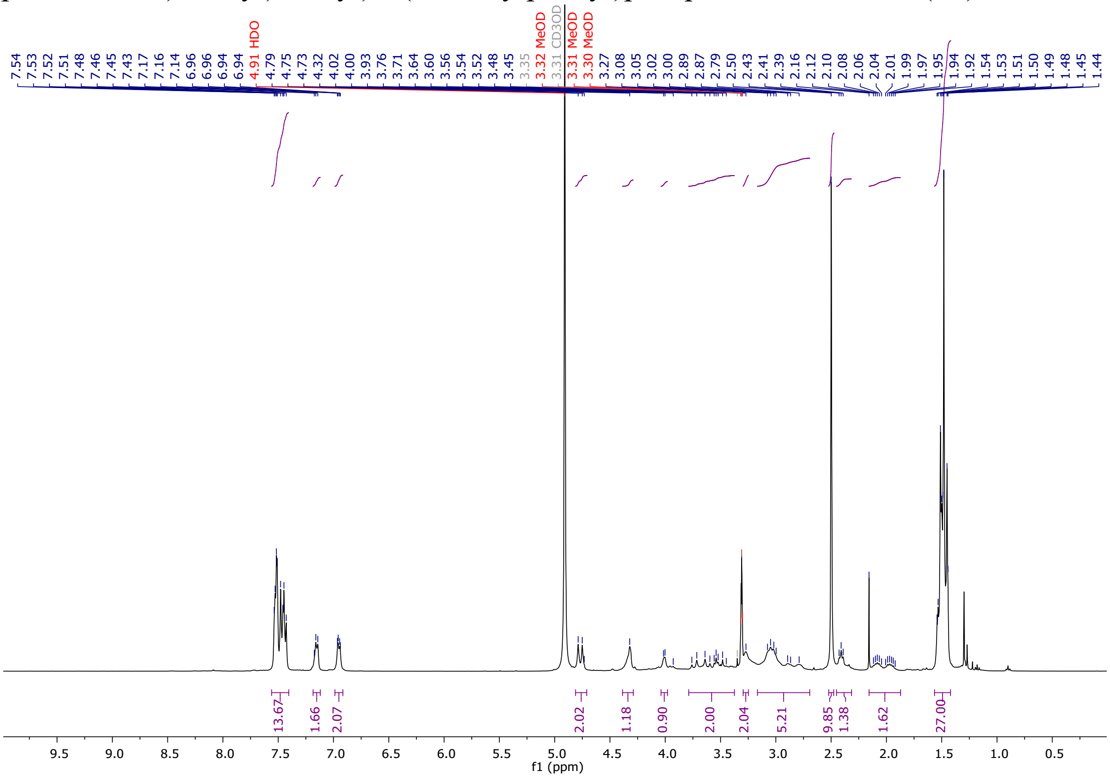

Figure S13: ^{1}H NMR spectrum (MeOD, 400 MHz, 298 K).

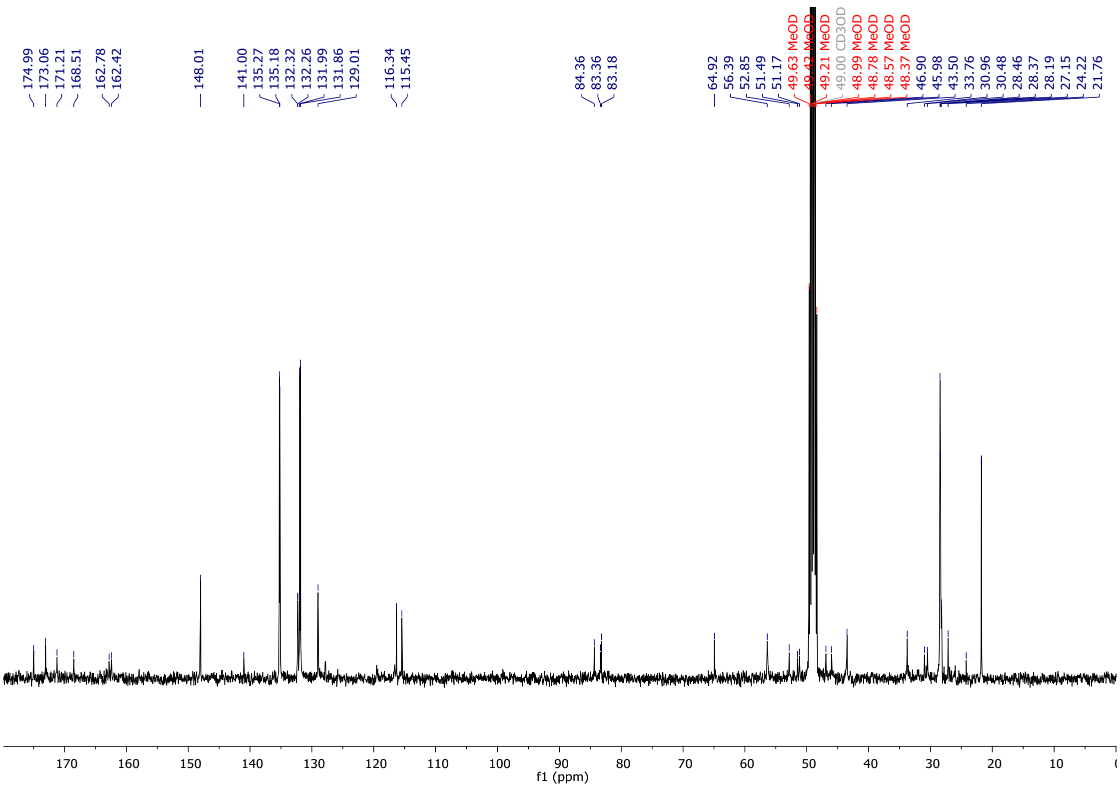

Figure S14: $^{13}C\{^{1}H\}$ NMR spectrum (MeOD, 100 MHz, 298 K).

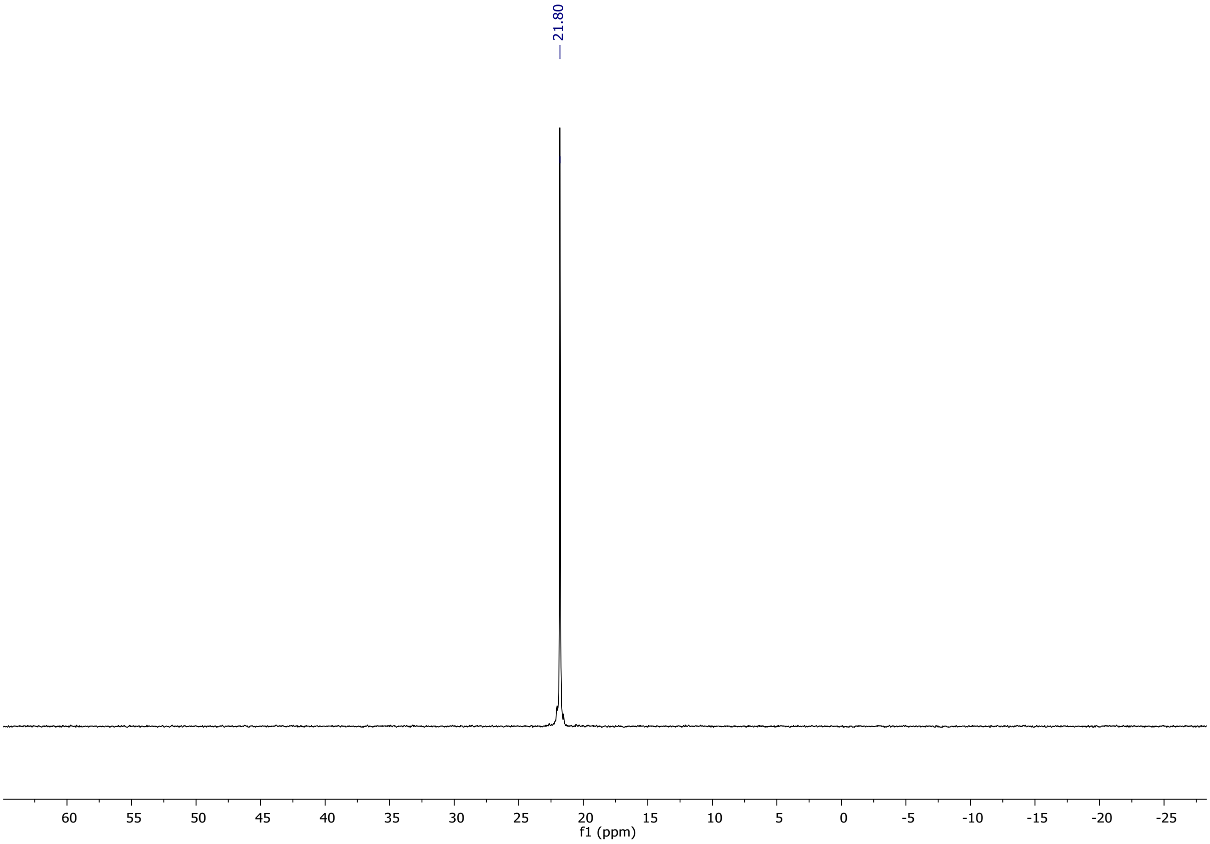

Figure S15: $^{31}P\{^{1}H\}$ NMR spectrum (MeOD, 162 MHz, 298 K).

(4-((4-(4,7-Bis(2-(*tert*-butoxy)-2-oxoethyl)-1,4,7-triazonan-1-yl)-5-(*tert*-butoxy)-5-oxopentanamido)methyl)benzyl)tri(3,5-dimethylphenyl)phosphonium bromide (**3c**)

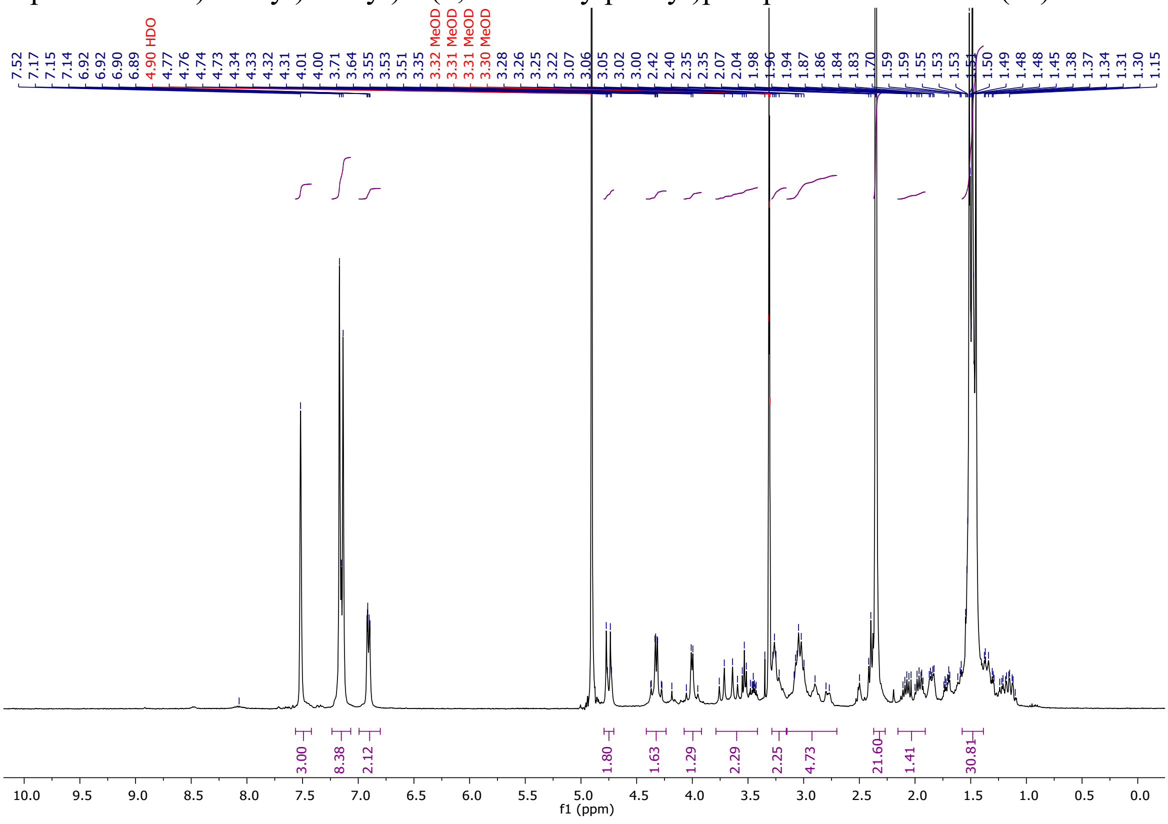

Figure S16: ^{1}H NMR spectrum (MeOD, 400 MHz, 298 K).

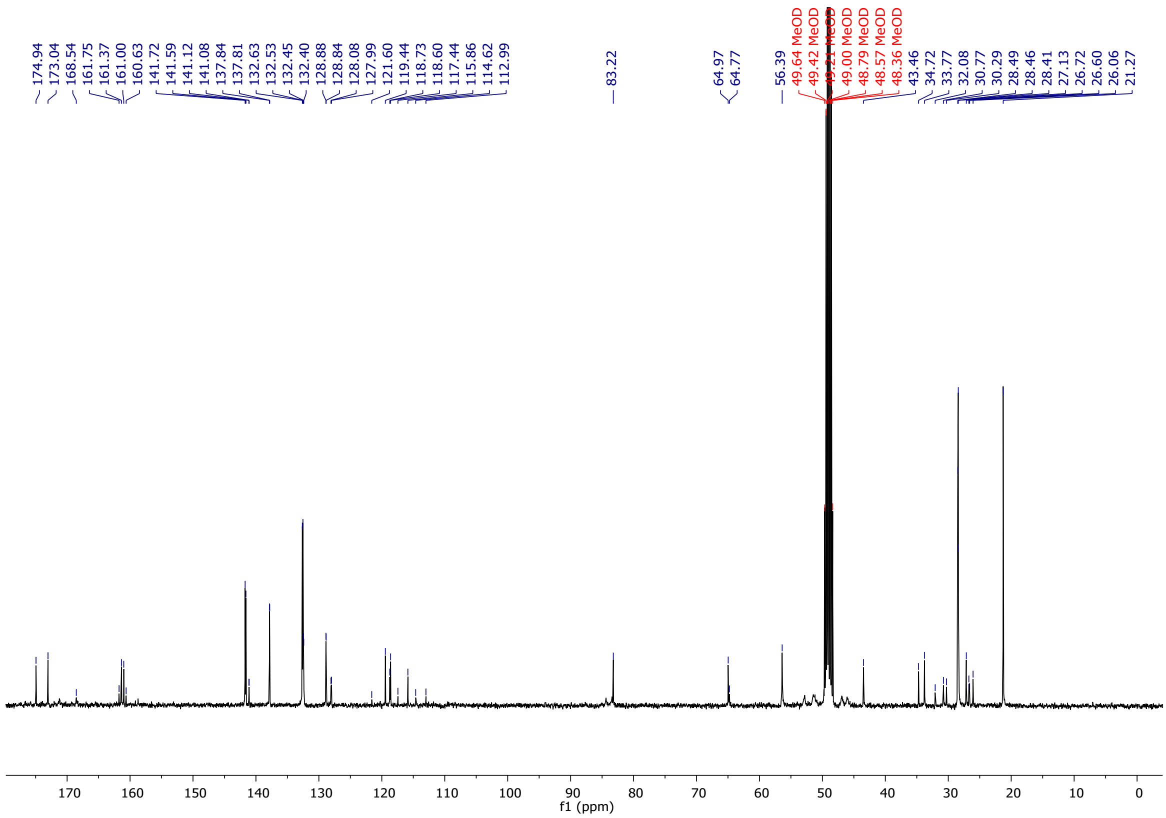

Figure S17: $^{13}C\{^{1}H\}$ NMR spectrum (MeOD, 100 MHz, 298 K).

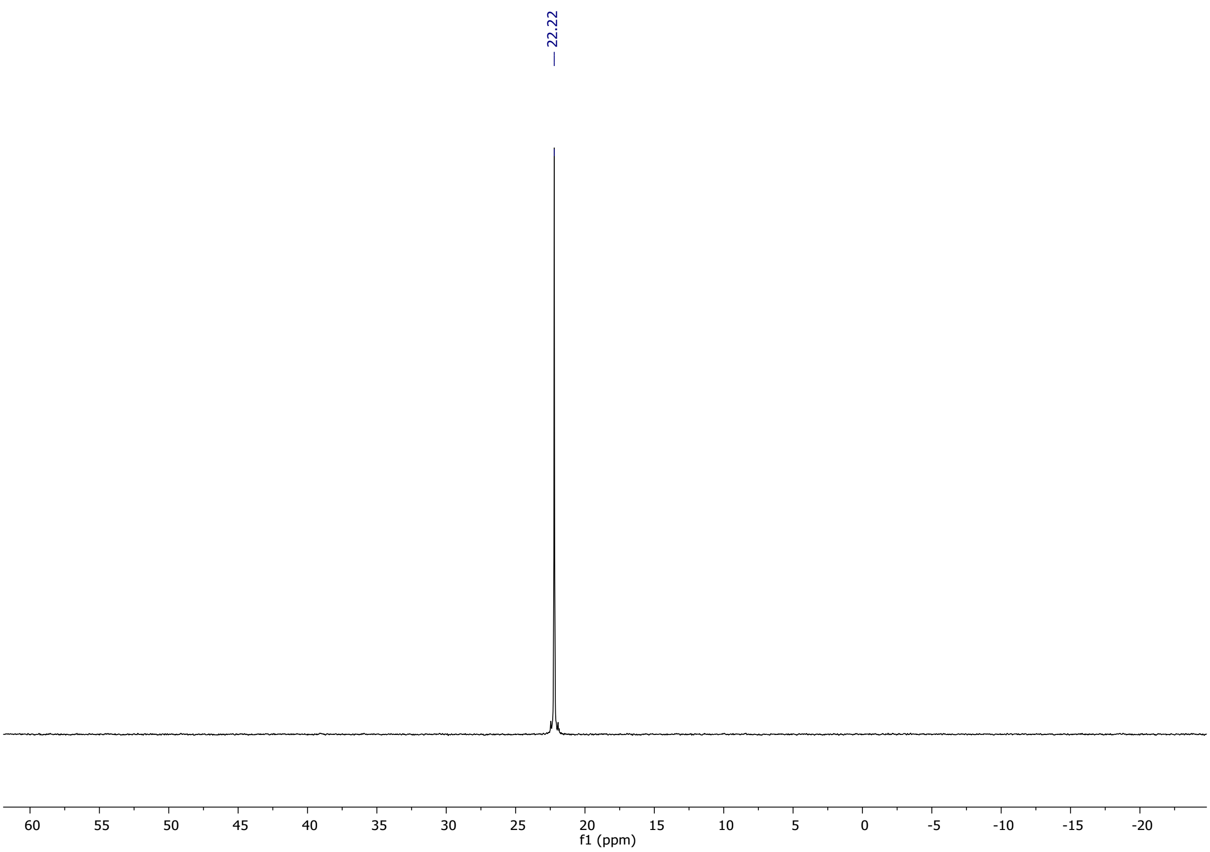

Figure S18: $^{31}P\{^{1}H\}$ NMR spectrum (MeOD, 162 MHz, 298 K).

NODAGA-xy-TPP Trifluoroacetate (**4a**)

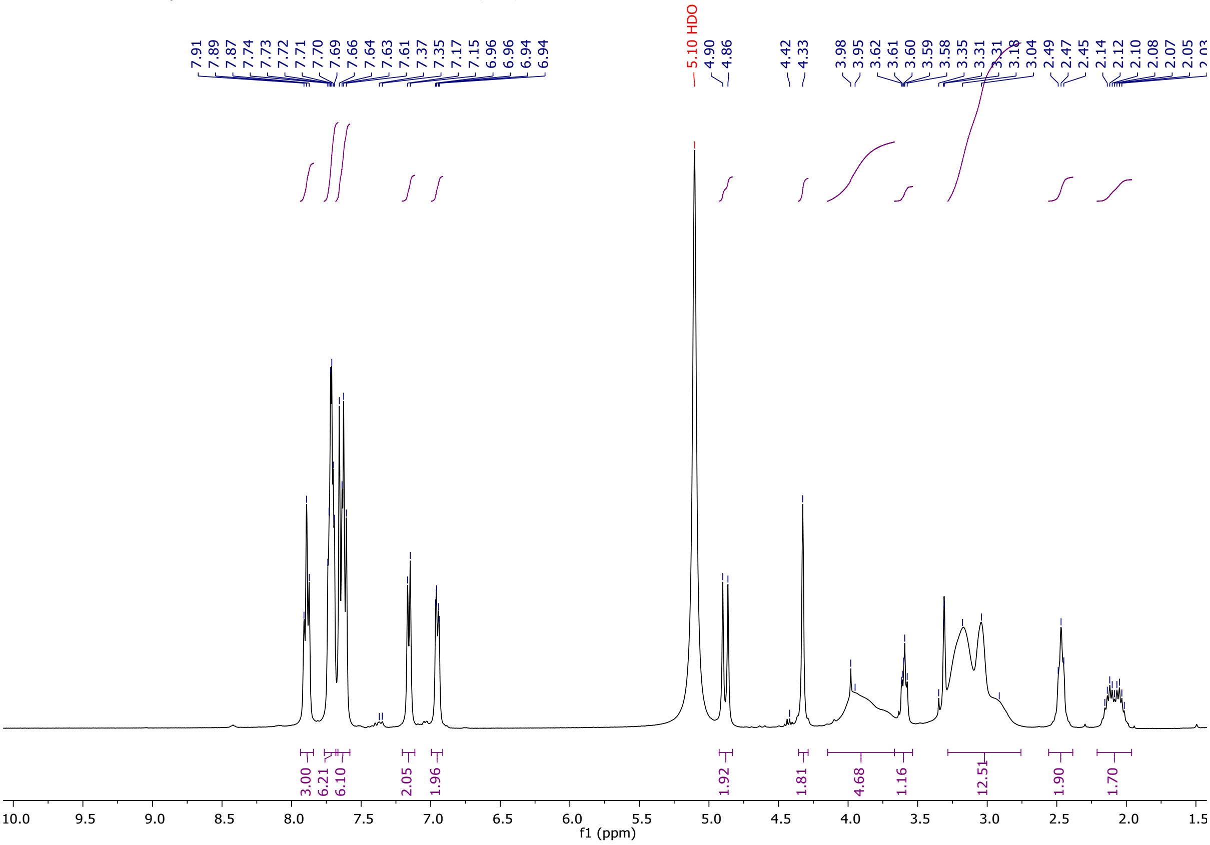

Figure S19: ^{1}H NMR spectrum (MeOD, 400 MHz, 298 K).

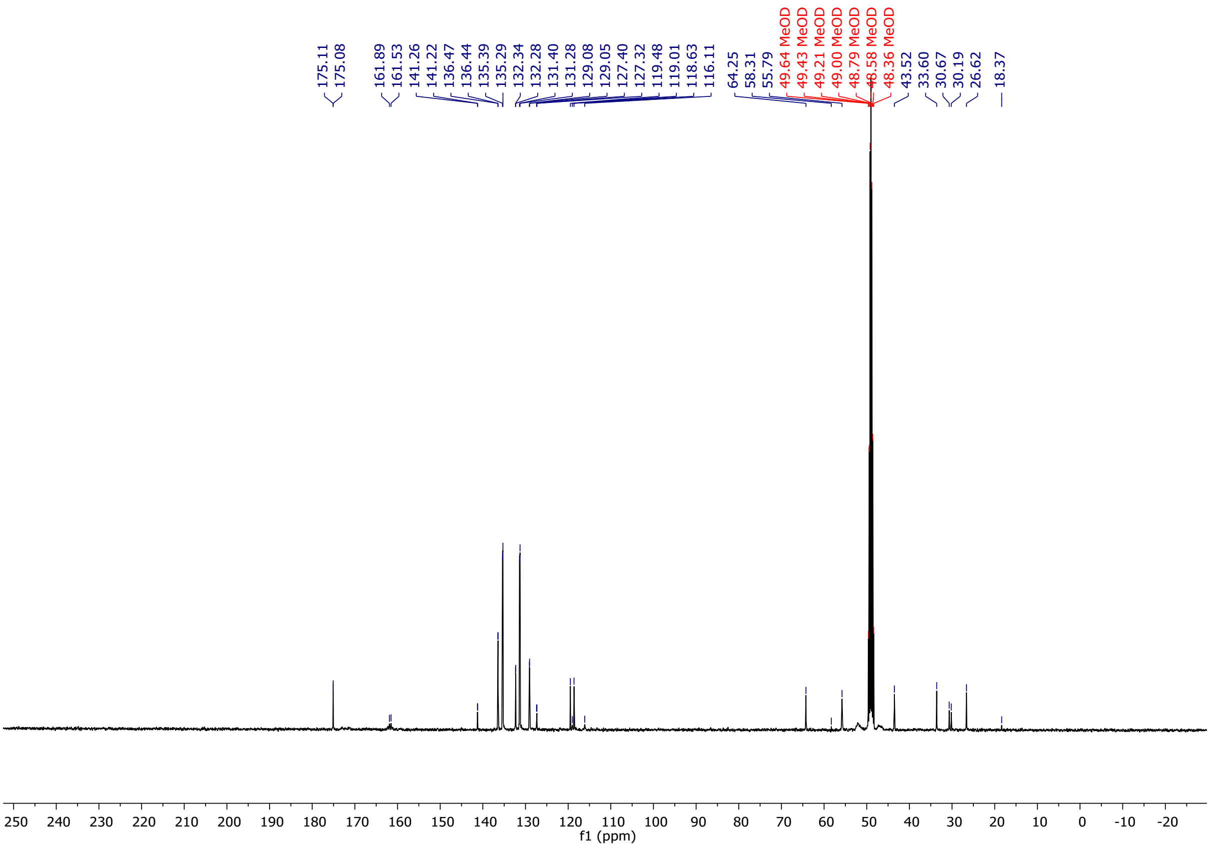

Figure S20: $^{13}C\{^{1}H\}$ NMR spectrum (MeOD, 100 MHz, 298 K).

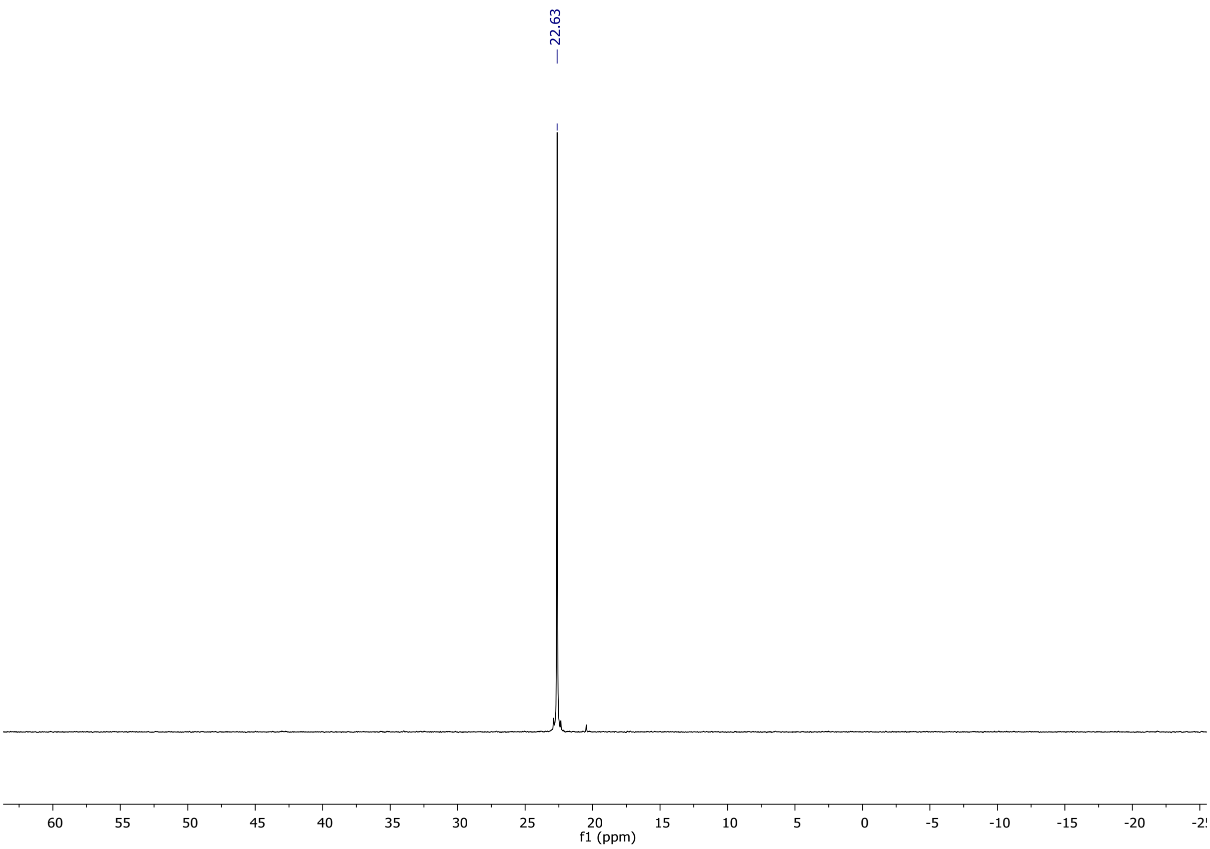

Figure S21: $^{31}P\{^1H\}$ NMR spectrum (MeOD, 162 MHz, 298 K).

NODAGA-xy-TTP Trifluoroacetate (**4b**)

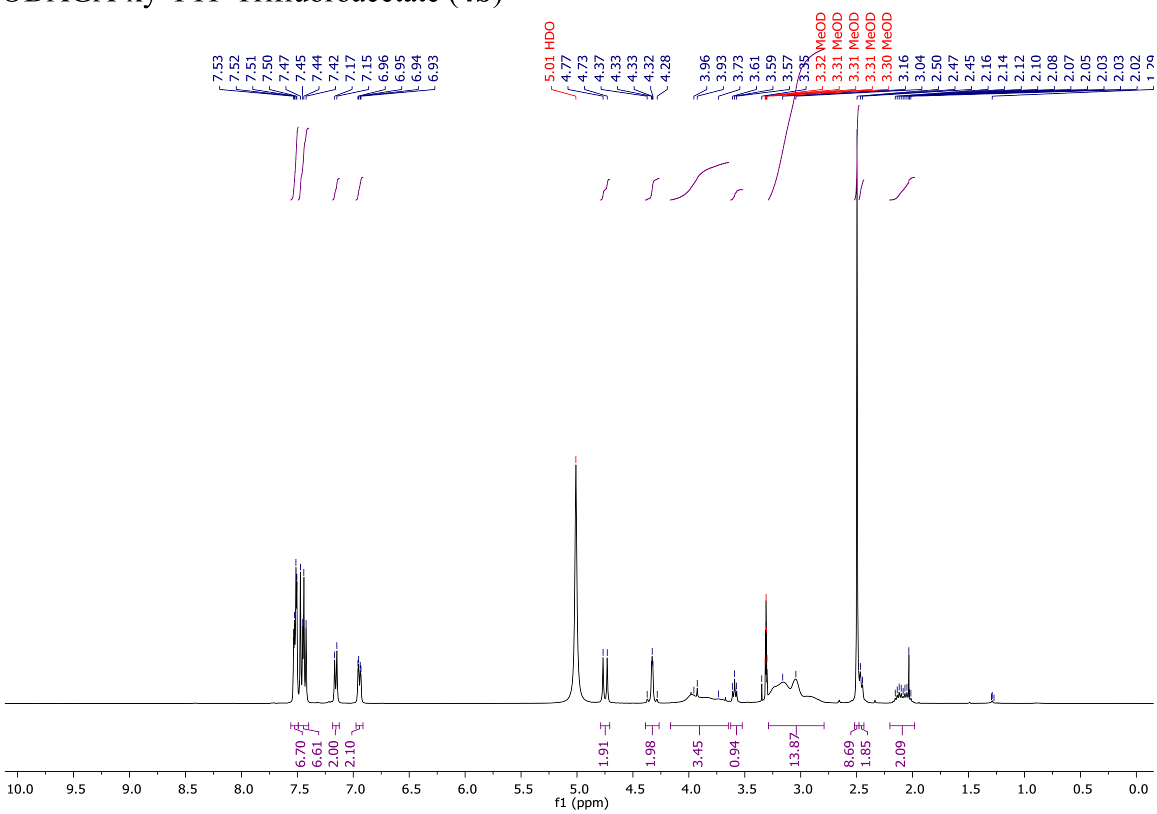

Figure S22: ^1H NMR spectrum (MeOD, 400 MHz, 298 K).

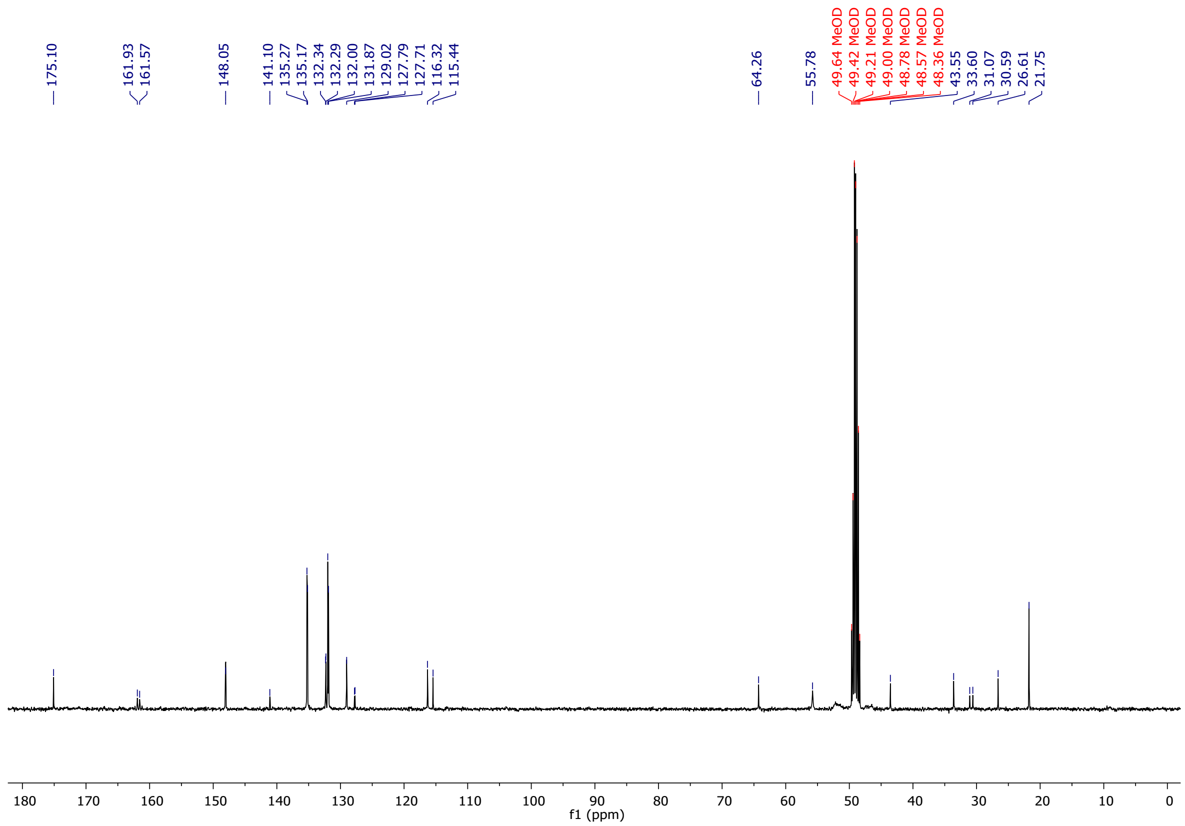

Figure S23: $^{13}C\{^{1}H\}$ NMR spectrum (MeOD, 100 MHz, 298 K).

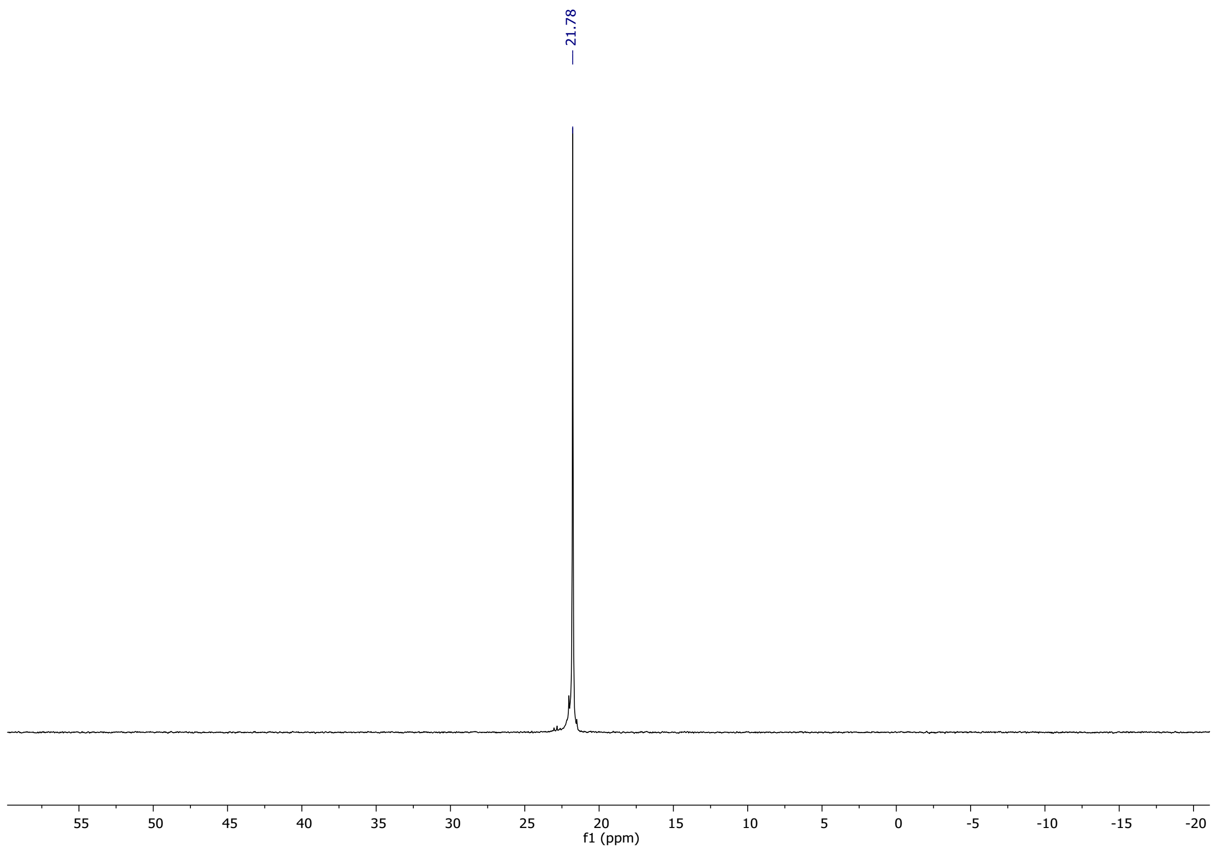

Figure S24: $^{31}P\{^{1}H\}$ NMR spectrum (MeOD, 162 MHz, 298 K).

NODAGA-xy-TXP Trifluoroacetate (**4c**)

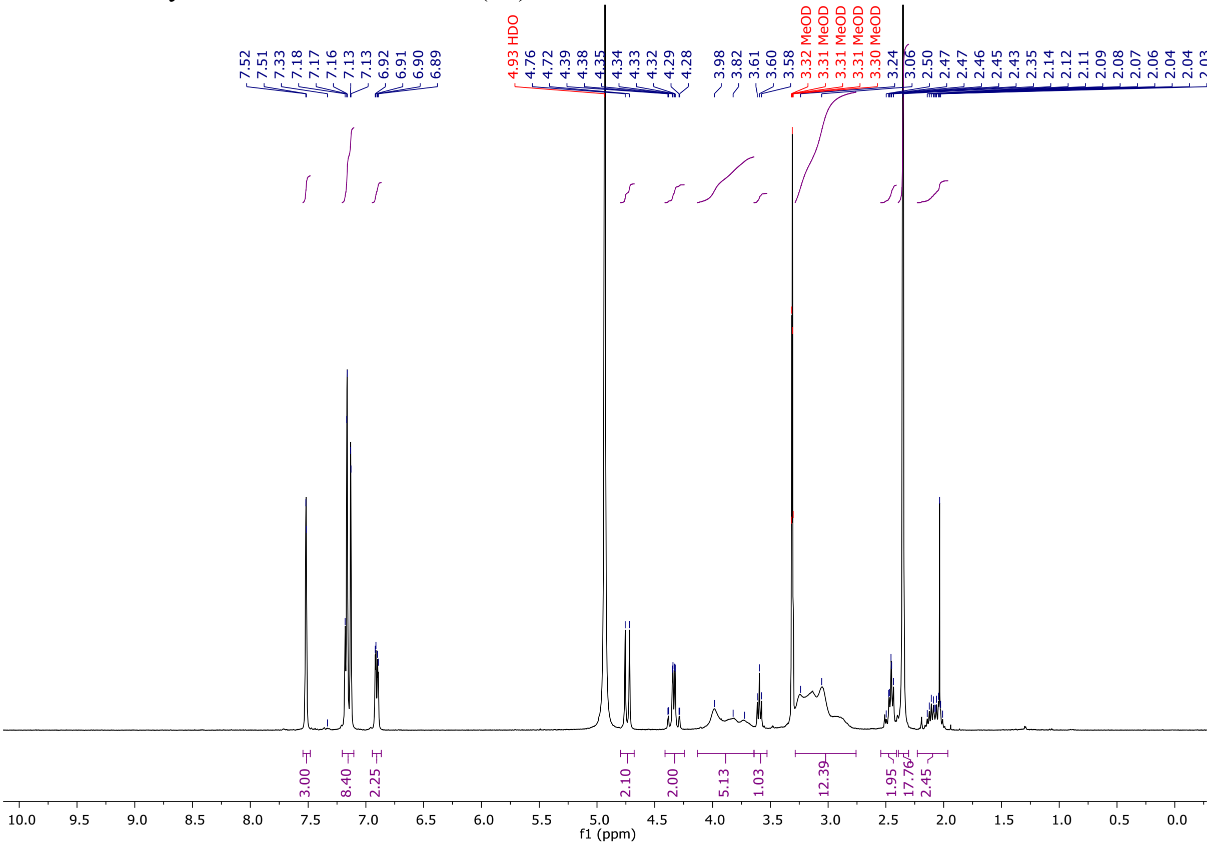

Figure S25: ^{1}H NMR spectrum (MeOD, 400 MHz, 298 K).

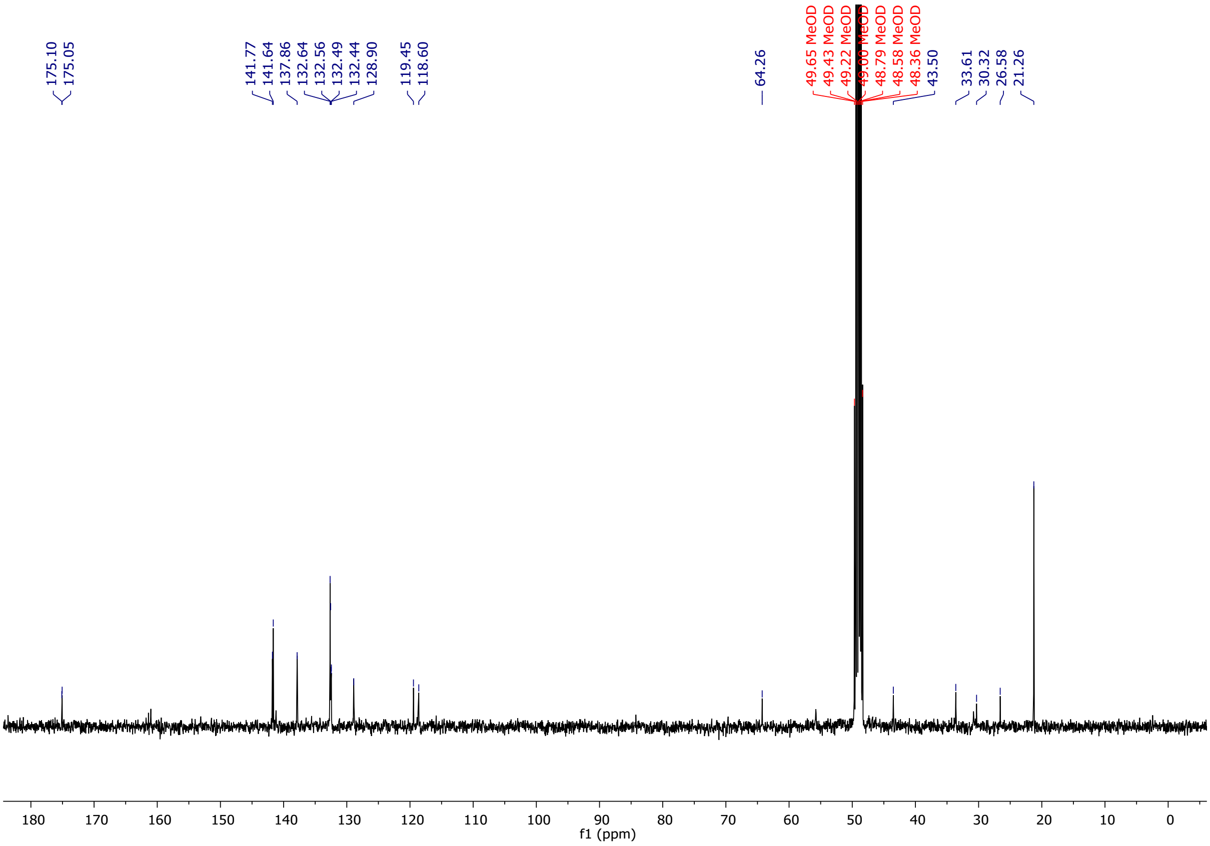

Figure S26: $^{13}C\{^{1}H\}$ NMR spectrum (MeOD, 100 MHz, 298 K).

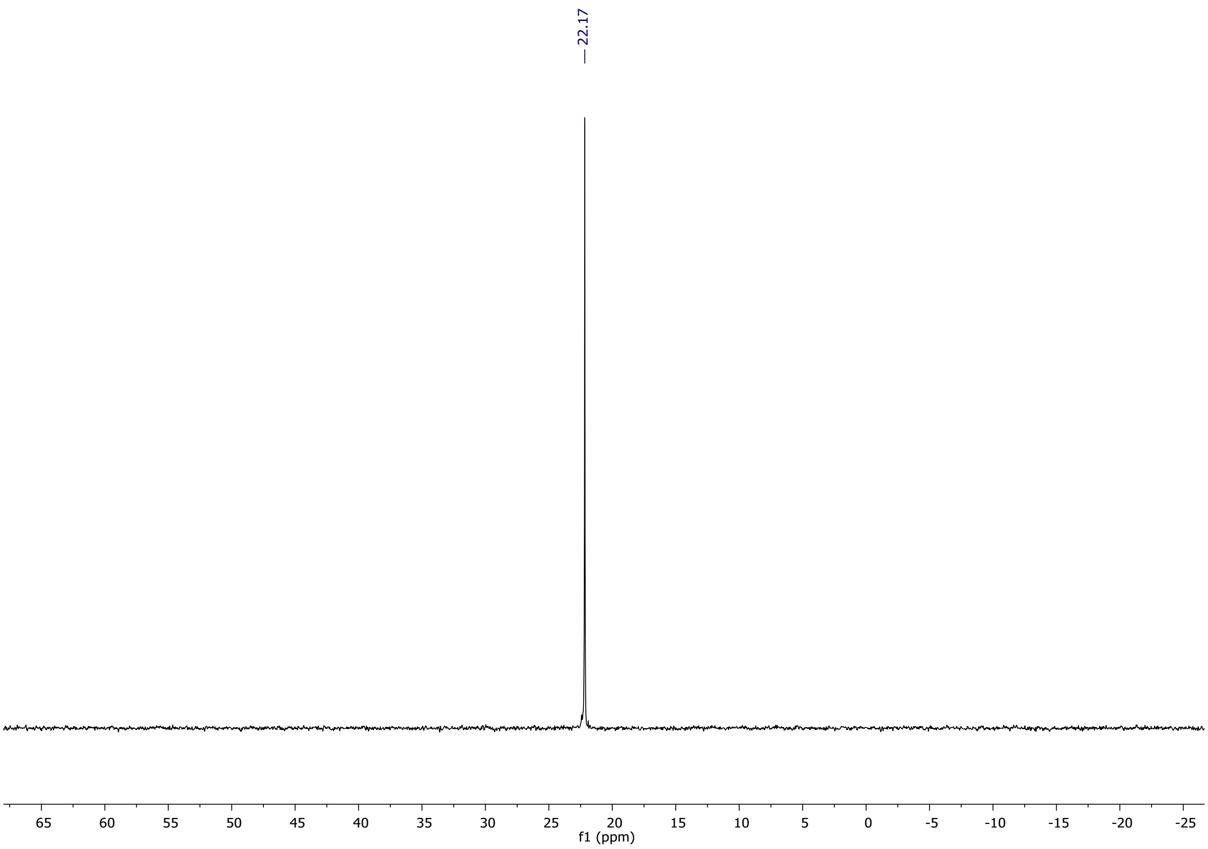

Figure S27: $^{31}P\{^{1}H\}$ NMR spectrum (MeOD, 162 MHz, 298 K).

[natGa]Ga-NODAGA-xy-TPP Trifluoroacetate (**[natGa]Ga4a**)

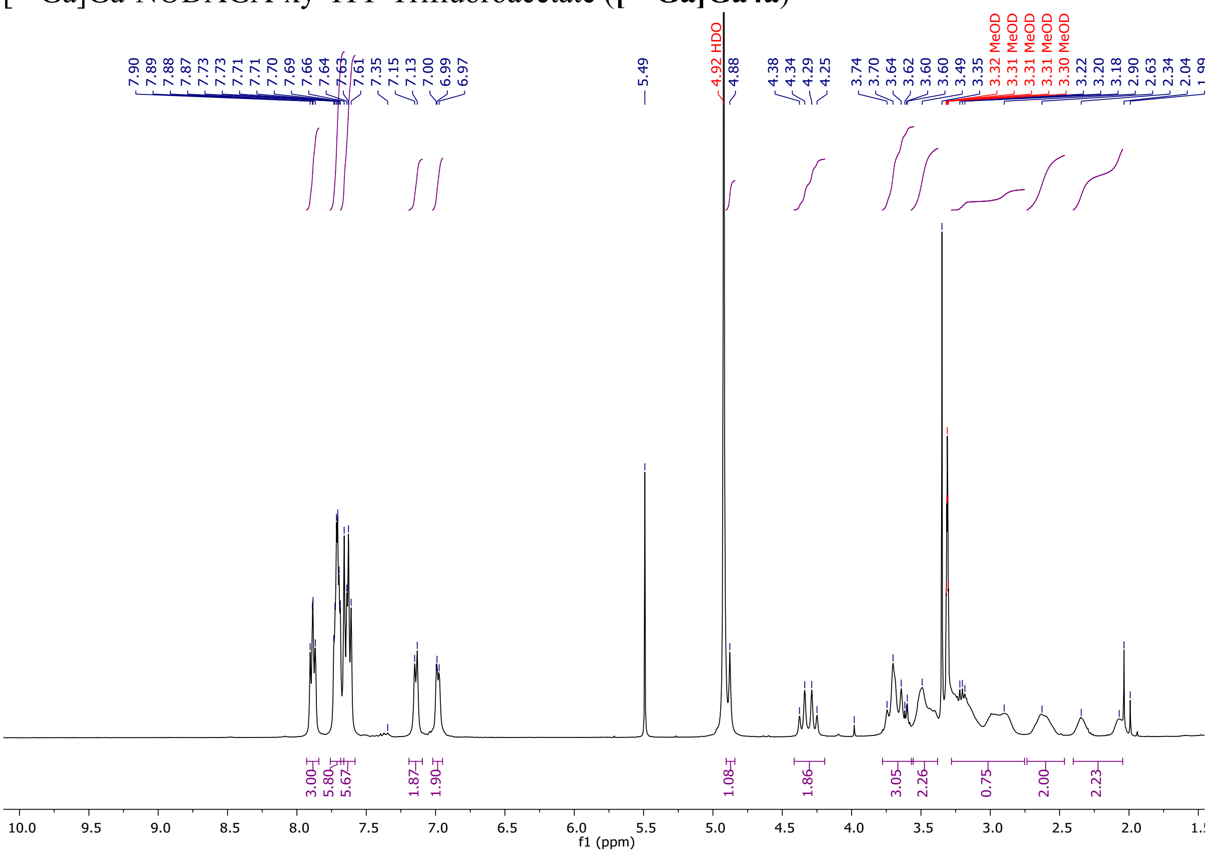

Figure S28: ^{1}H NMR spectrum (MeOD, 400 MHz, 298 K).

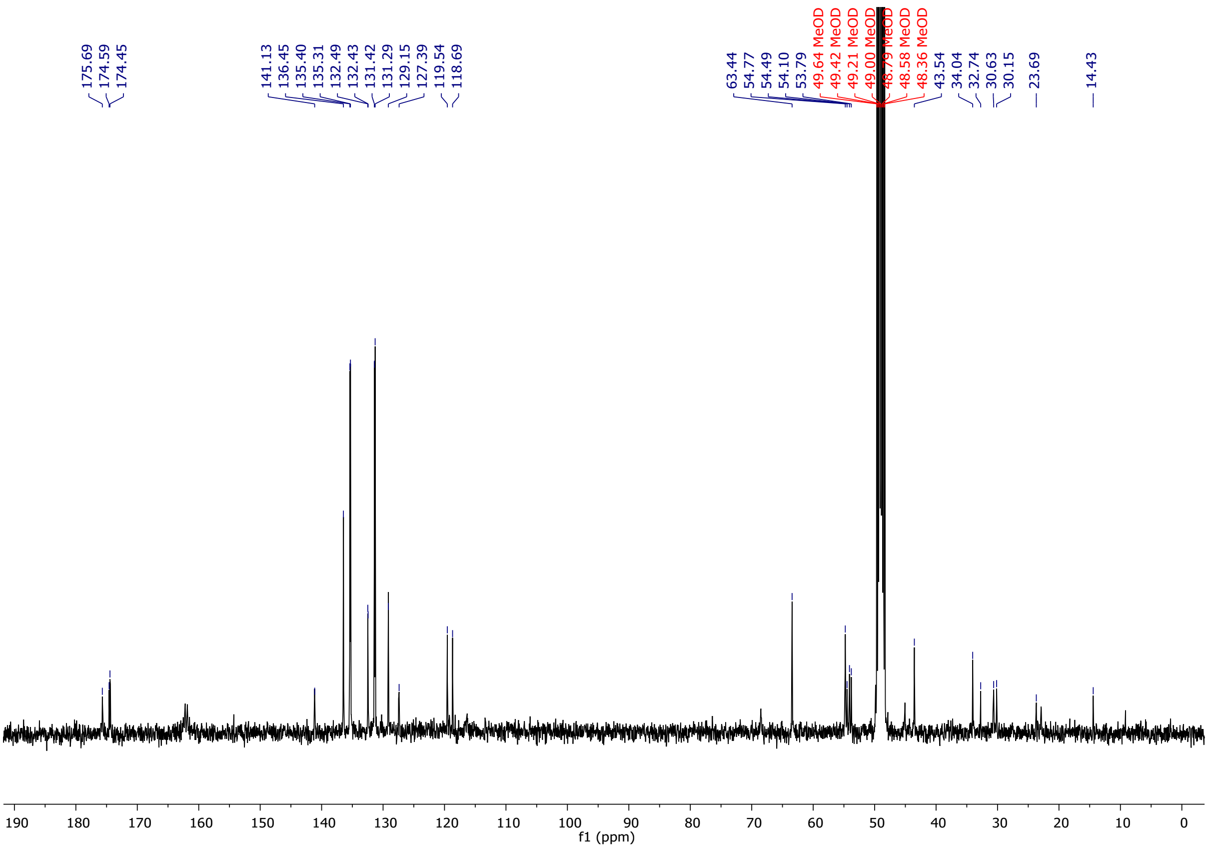

Figure S29: $^{13}C\{^{1}H\}$ NMR spectrum (MeOD, 100 MHz, 298 K).

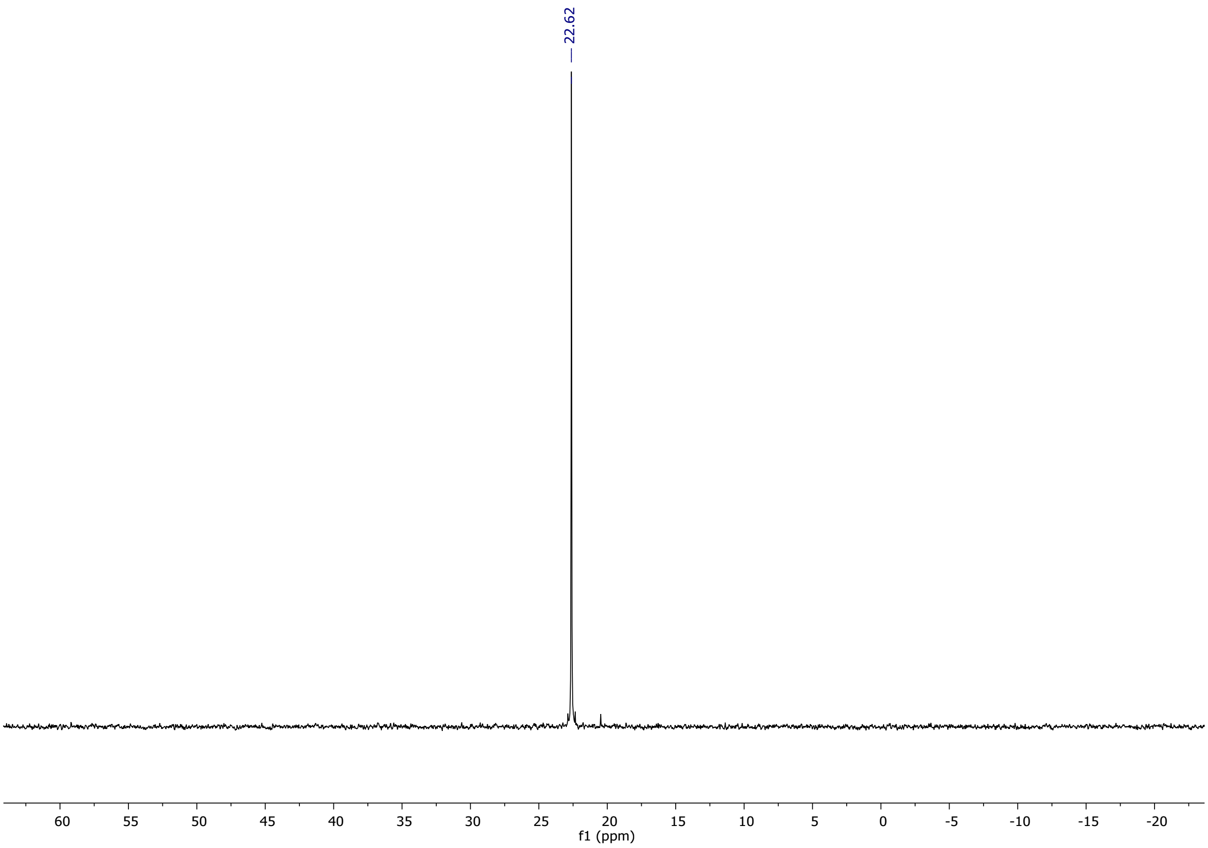

Figure S30: $^{31}P\{^{1}H\}$ NMR spectrum (MeOD, 162 MHz, 298 K).

[natGa]Ga-NODAGA-xy-TTP Trifluoroacetate (**[natGa]Ga4b**)

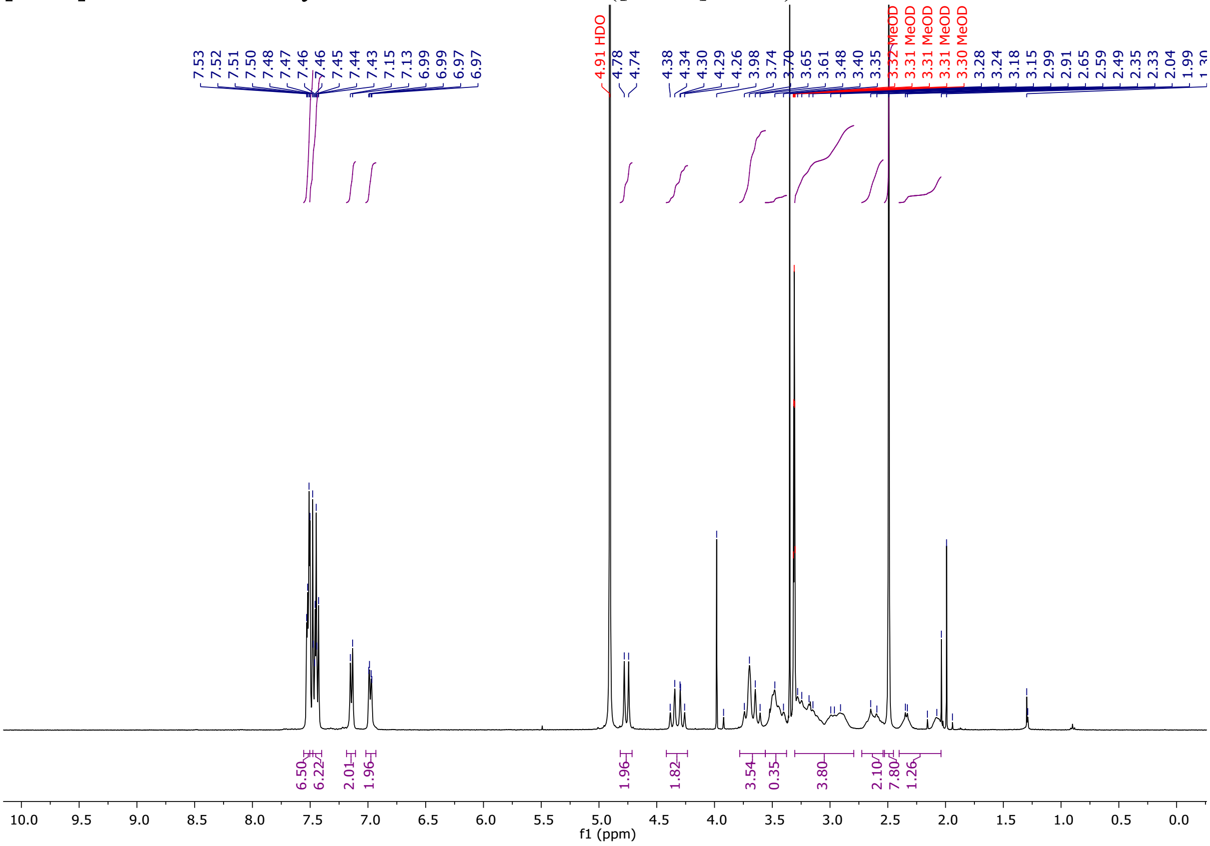

Figure S31: ^{1}H NMR spectrum (MeOD, 400 MHz, 298 K).

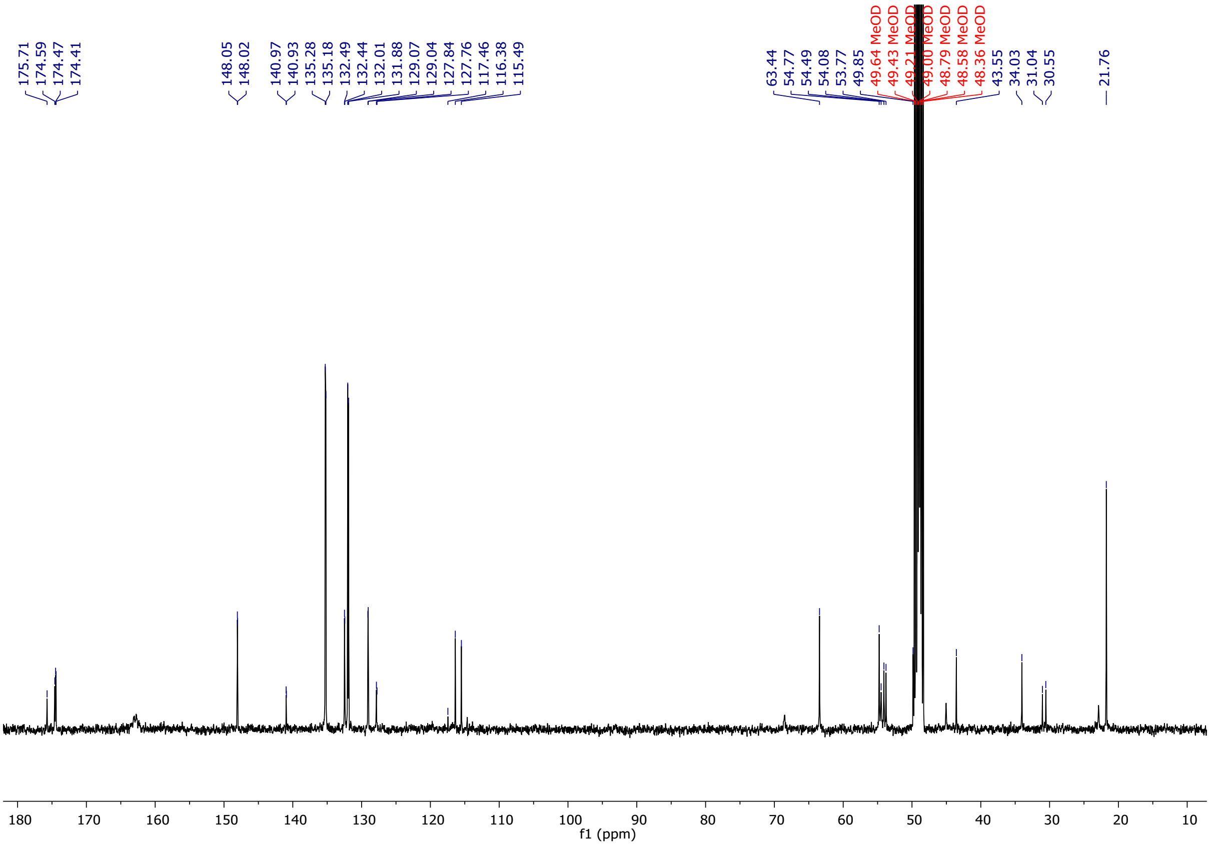

Figure S32: $^{13}C\{^{1}H\}$ NMR spectrum (MeOD, 100 MHz, 298 K).

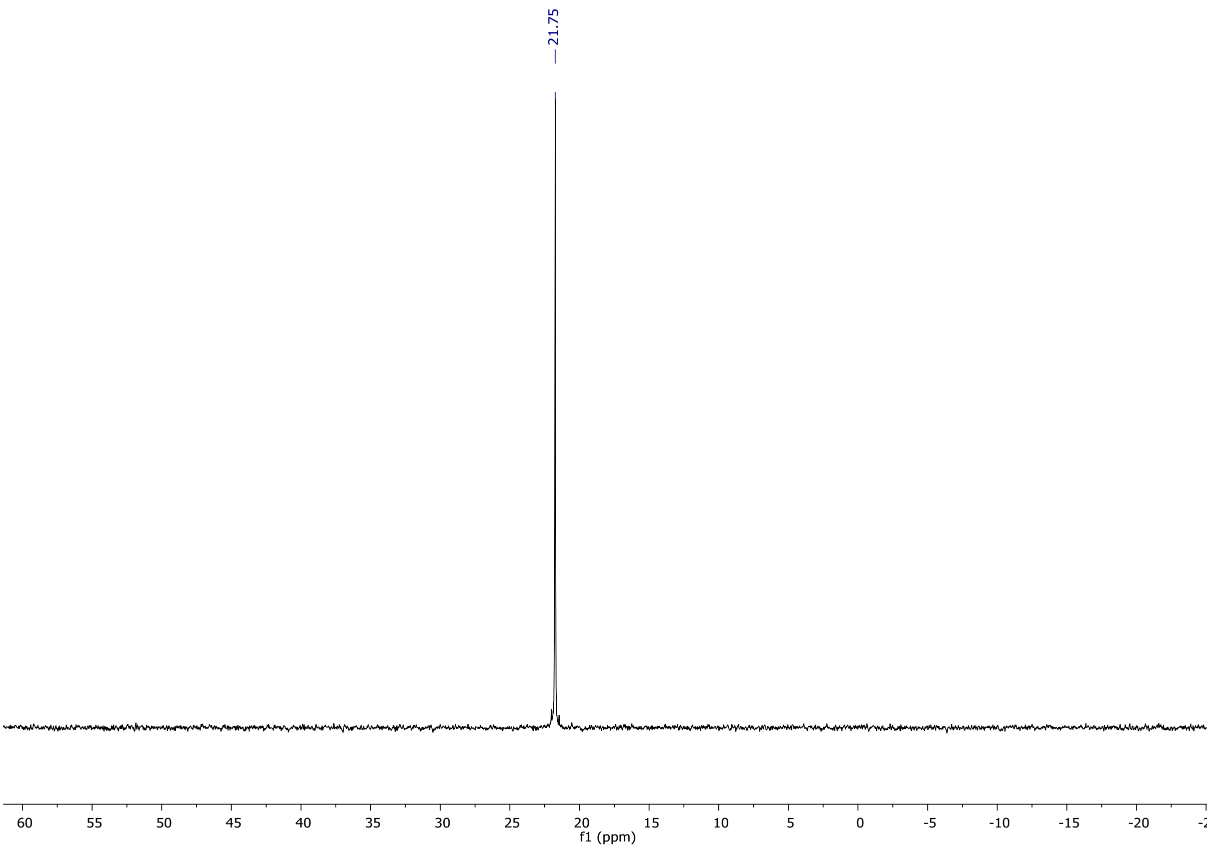

Figure S33: $^{31}P\{^{1}H\}$ NMR spectrum (MeOD, 162 MHz, 298 K).

[natGa]Ga-NODAGA-xy-TXP Trifluoroacetate (**[natGa]Ga4c**)

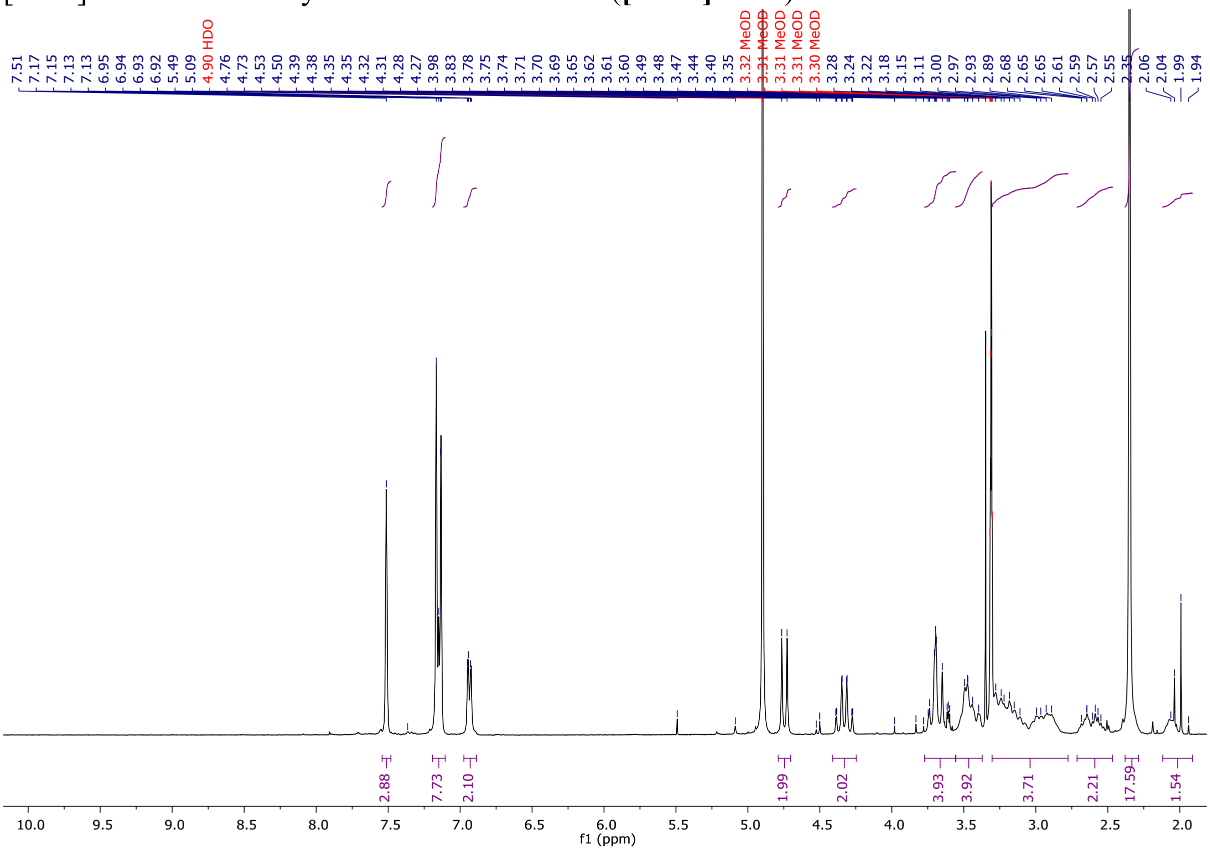

Figure S34: ^{1}H NMR spectrum (MeOD, 400 MHz, 298 K).

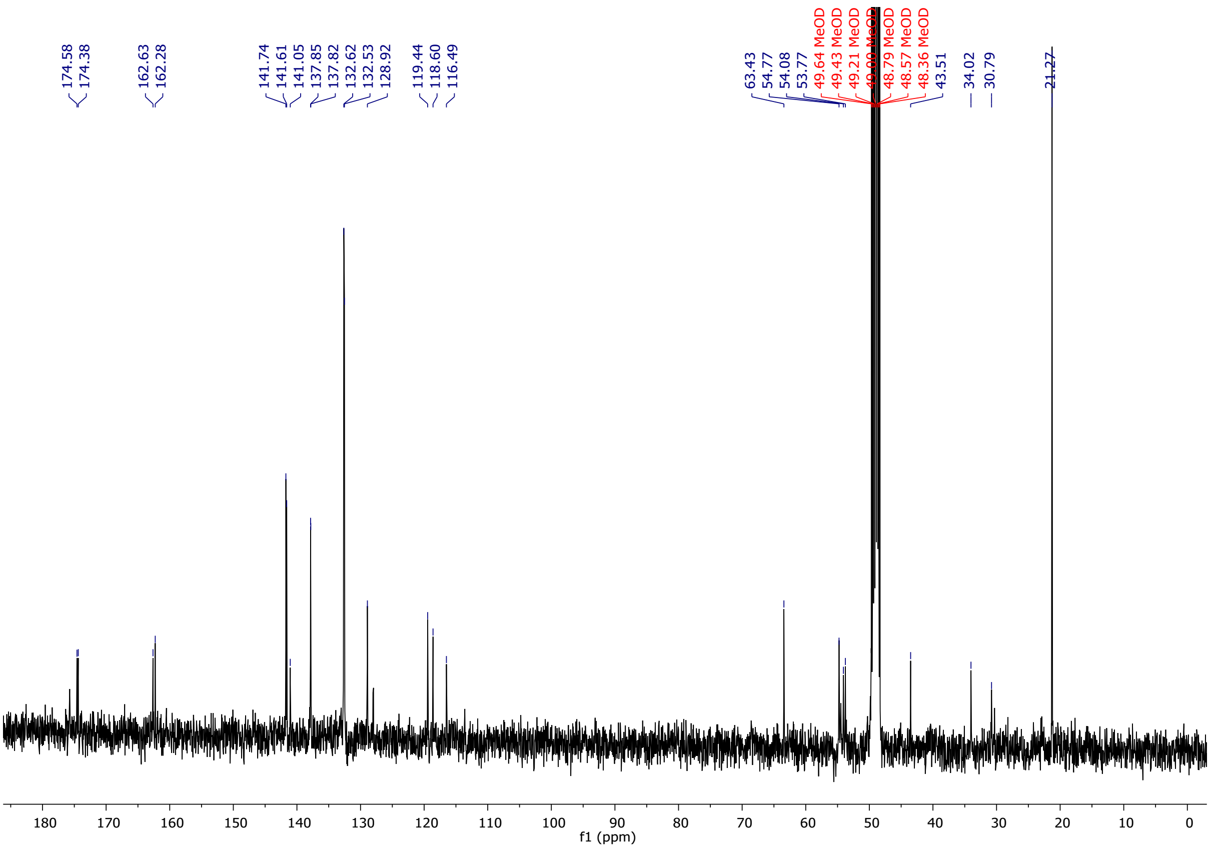

Figure S35: $^{13}C\{^{1}H\}$ NMR spectrum (MeOD, 100 MHz, 298 K).

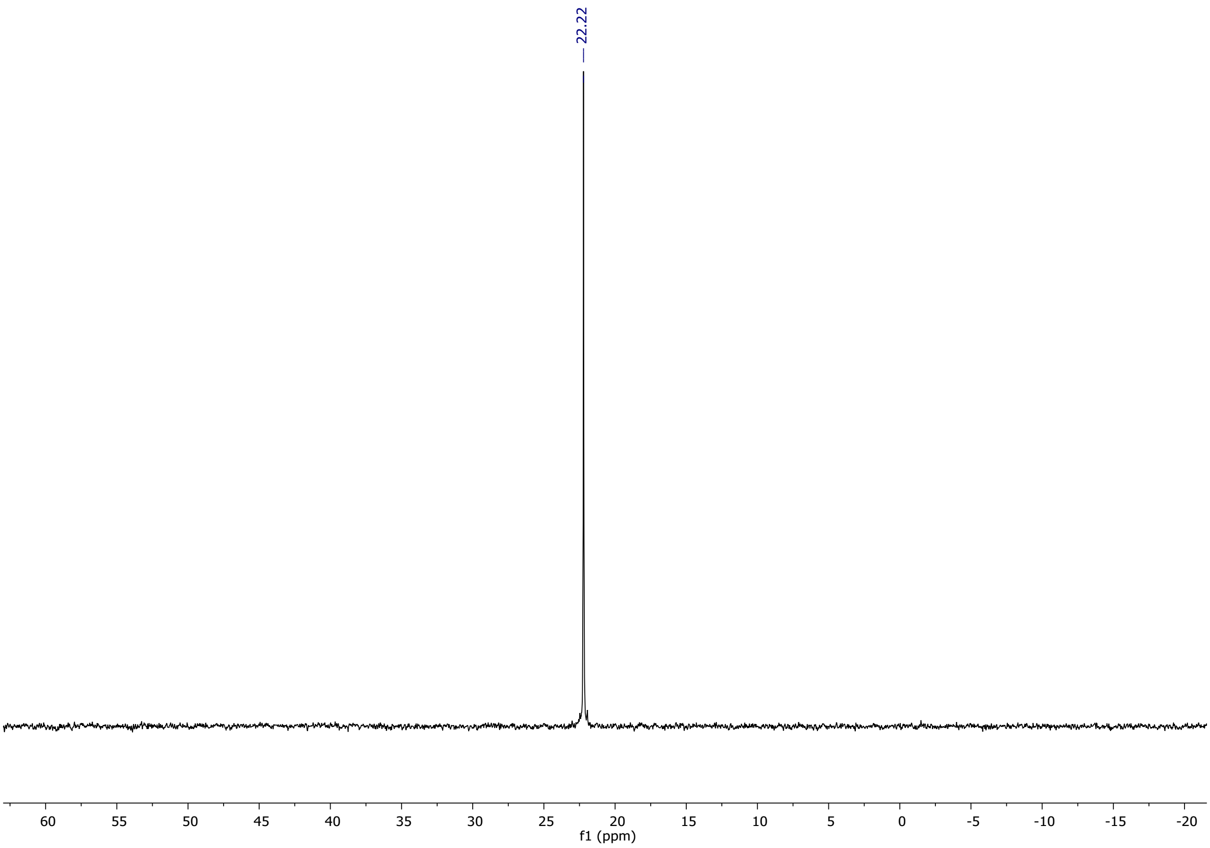

Figure S36: $^{31}P\{^{1}H\}$ NMR spectrum (MeOD, 162 MHz, 298 K).

iTLC Analysis

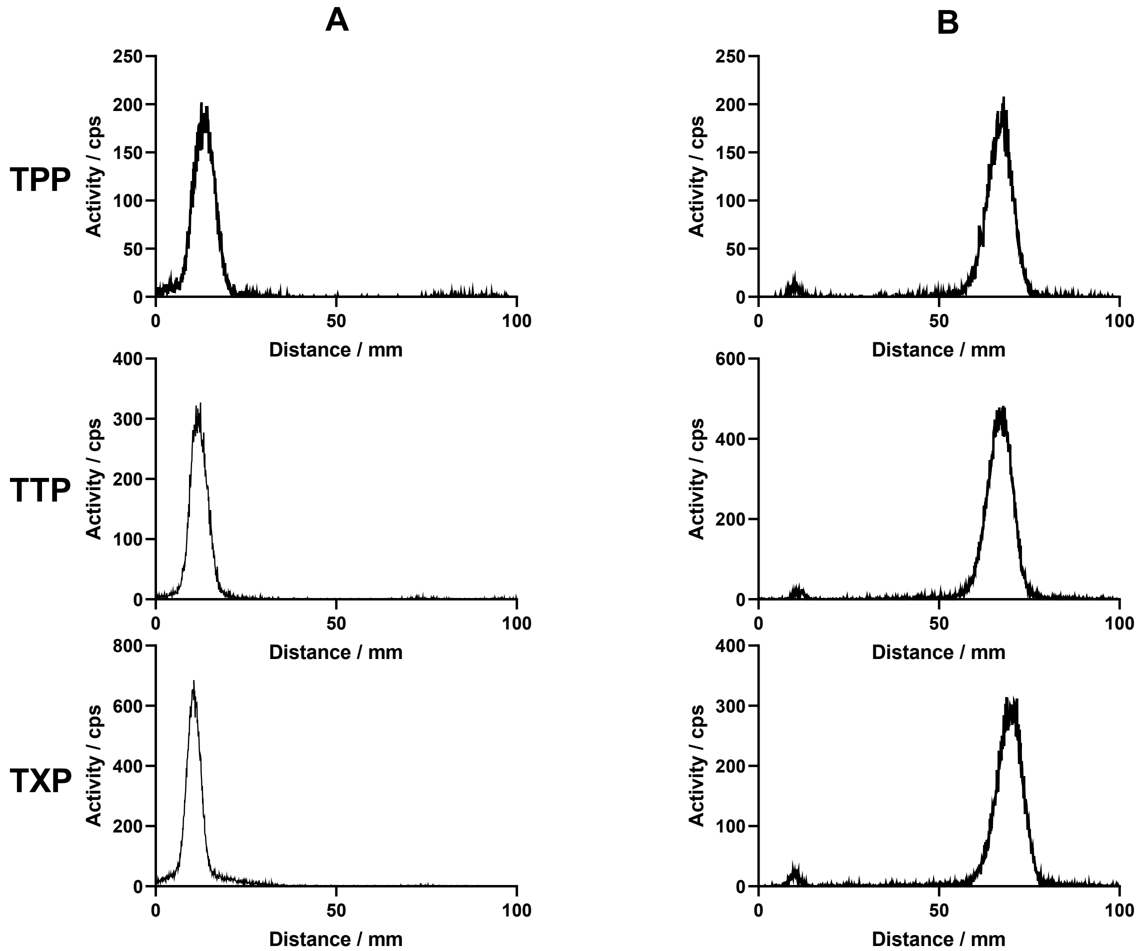

Figure S37: iTLC traces of [^{68}Ga]Ga-NODAGA-xy-TPP, [^{68}Ga]Ga-NODAGA-xy-TTP, [^{68}Ga]Ga-NODAGA-xy-TXP. (A) Mobile phase: 0.1 M disodium EDTA. (B) Mobile phase: 2.0 M NH_4OAc:MeOH (1:1).

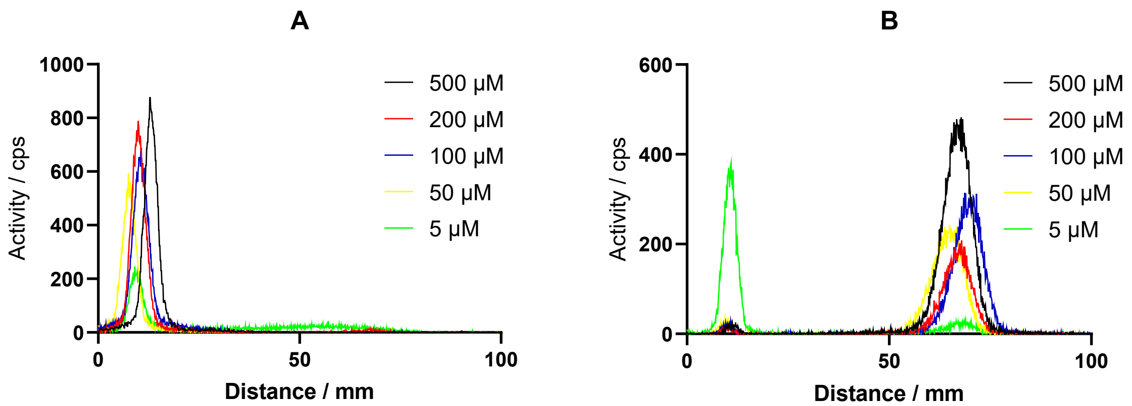

Figure S38: Dilution study iTLC traces of [^{68}Ga]Ga-NODAGA-xy-TXP at ligand concentrations of 500 µM (black), 200 µM (red), 100 µM (blue), 50 µM (yellow) and 5 µM (green). (A) Mobile phase: 0.1 M disodium EDTA. (B) Mobile phase: 2.0 M NH_4OAc:MeOH (1:1).

RadioHPLC Analysis

[68Ga]Ga-NODAGA-xy-TPP (**[68Ga]Ga4a**)

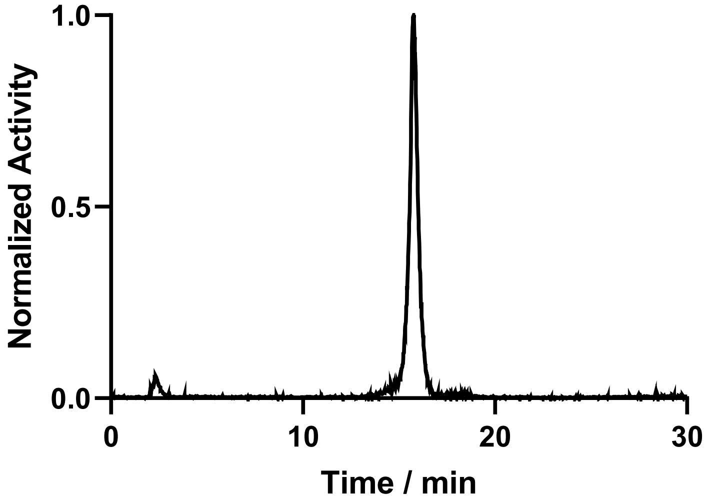

Figure S39: RadioHPLC trace of [68Ga]Ga-NODAGA-xy-TPP. Eluent gradient: water (0.1 % TFA) (A) and MeCN (0.1 % TFA) (B) (95 % A for 5 min, 0 – 95 % B in A for 20 min, 95 % B for 5 min; flow rate 1 mL min^{-1}).

[68Ga]Ga-NODAGA-xy-TTP (**[68Ga]Ga4b**)

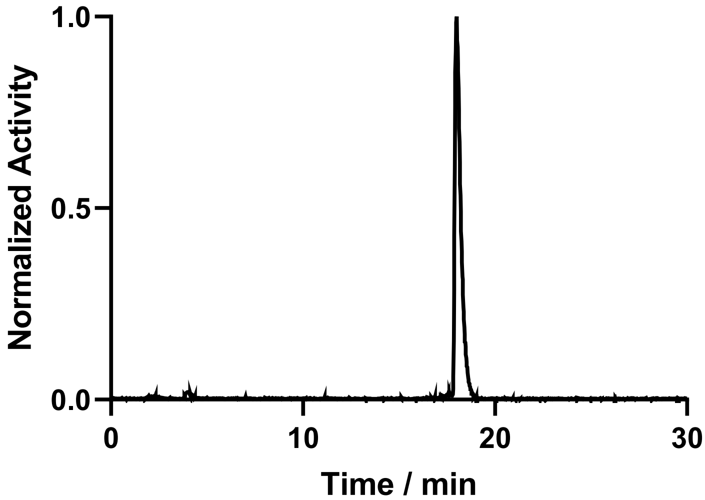

Figure S40: RadioHPLC trace of [68Ga]Ga-NODAGA-xy-TTP. Eluent gradient as described for Figure S39.

[^{68}Ga]Ga-NODAGA-xy-TXP (**[^{68}Ga]Ga4c**)

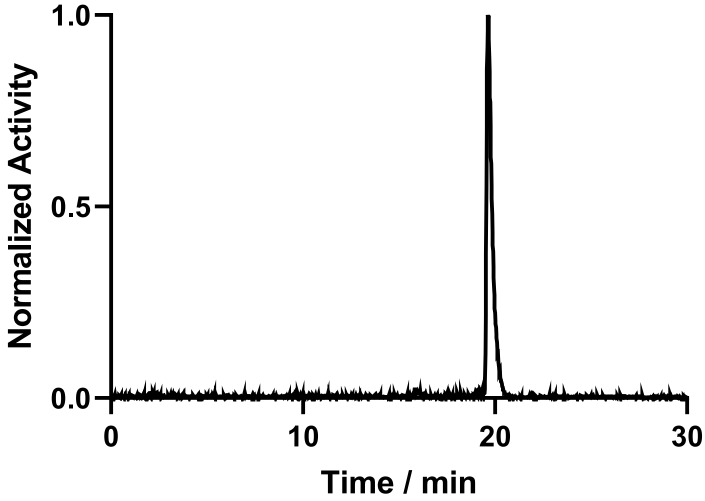

Figure S41: RadioHPLC trace of [^{68}Ga]Ga-NODAGA-xy-TXP. Eluent gradient as described for Figure S39.

Langendorff Isolated Heart Perfusion

Stability Study

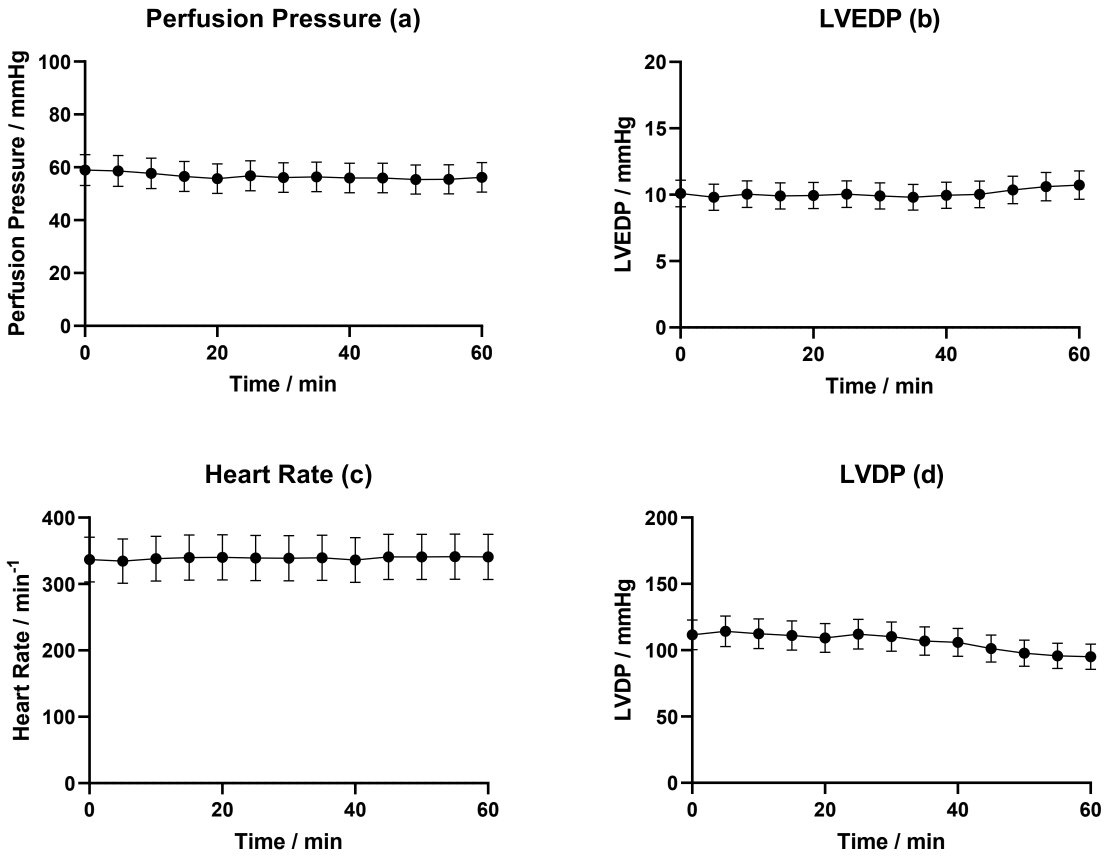

Figure S42: Stability study performed to generate exclusion criteria for the function of isolated perfused hearts. **(a)** perfusion pressure, **(b)** left ventricular end-diastolic pressure (LVEDP), **(c)** heart rate, **(d)** left ventricular developed pressure (LVDP). Perfusion pressure was measured by a pressure transducer connected to the arterial line, whilst LVEDP, LVDP and heart rate were calculated as a function of the left ventricular pressure measured by an isovolumetric balloon connected to a pressure transducer inserted into the left ventricle. Hearts were electrically paced at 340 min^{-1}. Data represents (n = 6) ± SD.

Effects of 600 nM CCCP Infusion on Haemodynamic Parameters

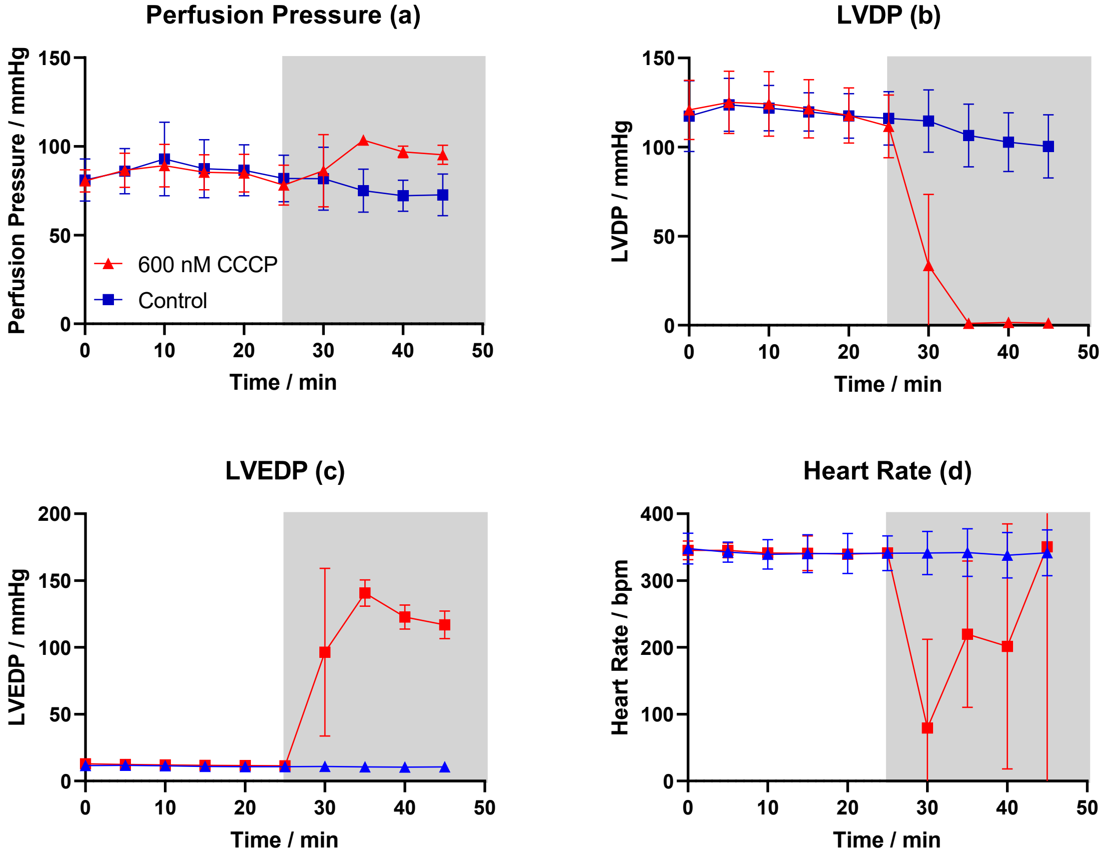

Figure S43: Haemodynamic parameters for control hearts undergoing normal function for 45 minutes (n = 6, blue) and hearts undergoing normal function for 25 minutes followed by infusion with 600 nM CCCP for 20 minutes (n = 6, red). **(a)** perfusion pressure, **(b)** LVDP, **(c)** LVEDP, **(d)** heart rate. Data represents mean ± SD.

Triple γ-Detector System Raw Data for [^{99m}Tc]Tc-sestaMIBI Using the Two-Injection Protocol

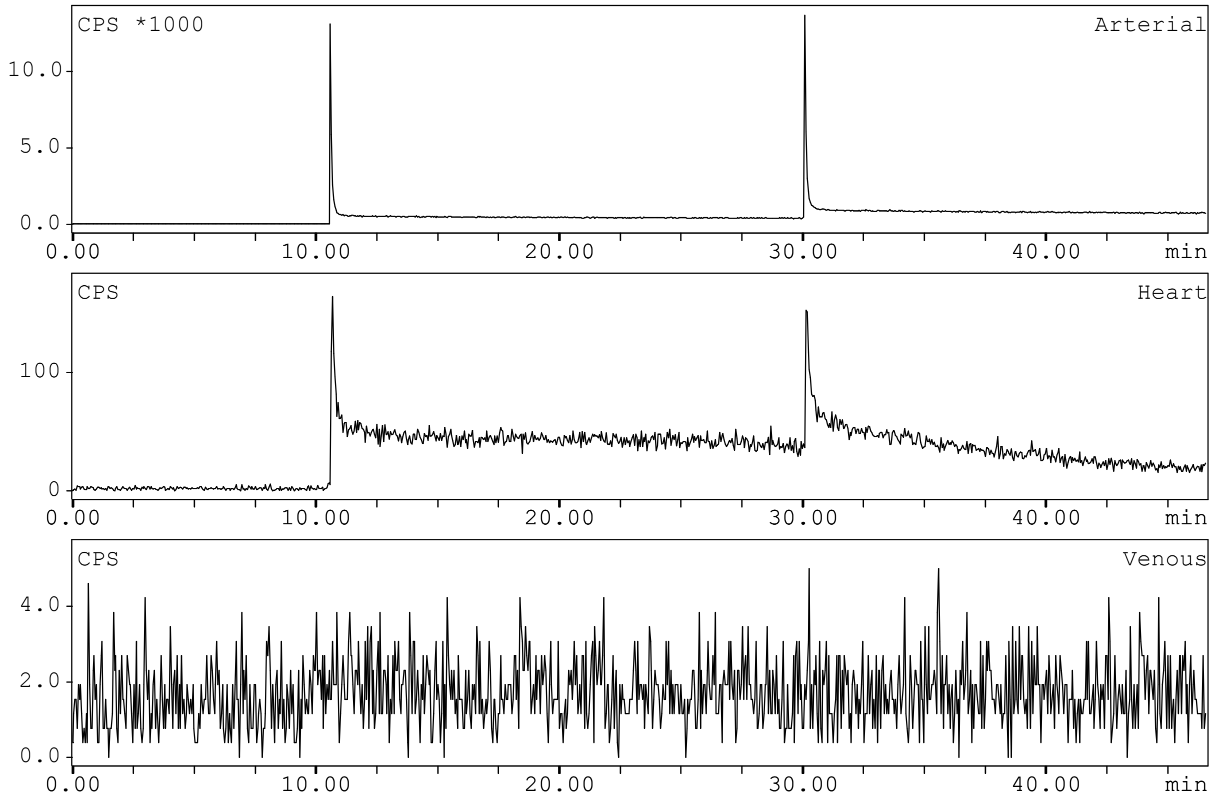

Figure S44: Experiment 1. There was an issue with the venous detector and as such an accurate venous trace could not be obtained.

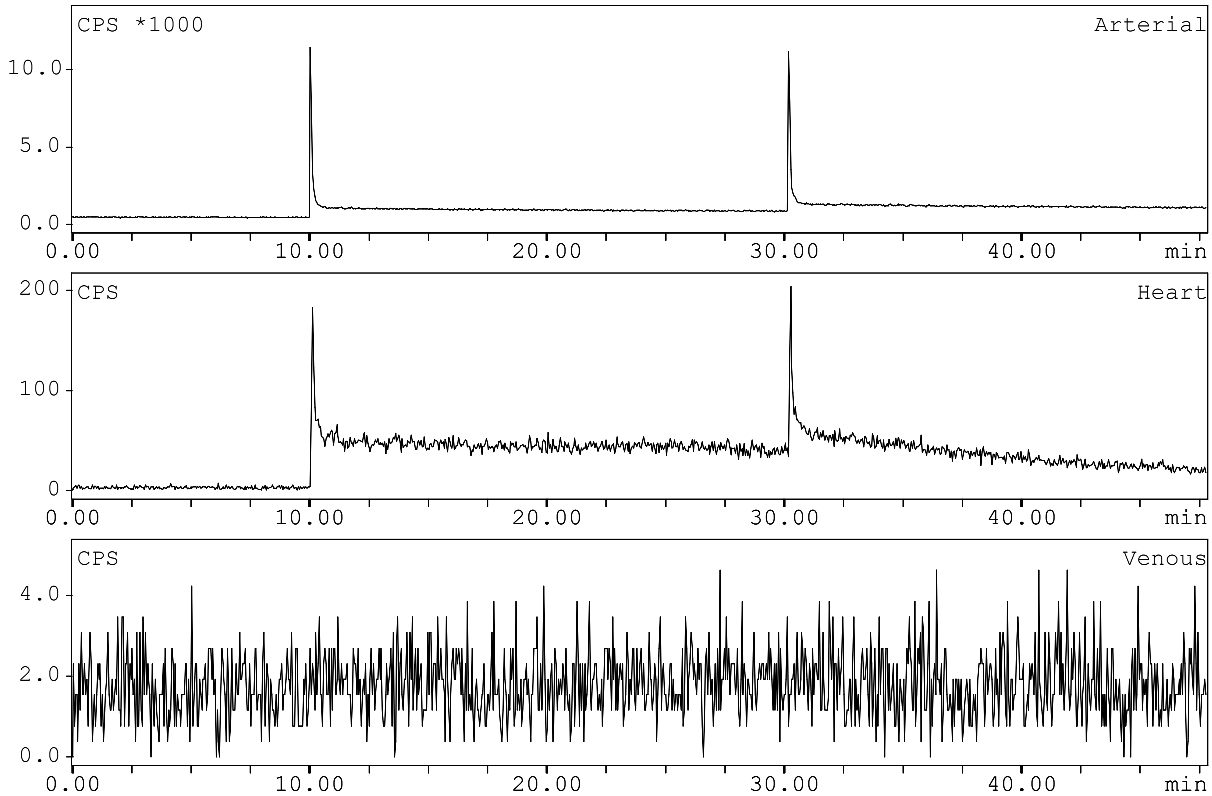

Figure S45: Experiment 2.

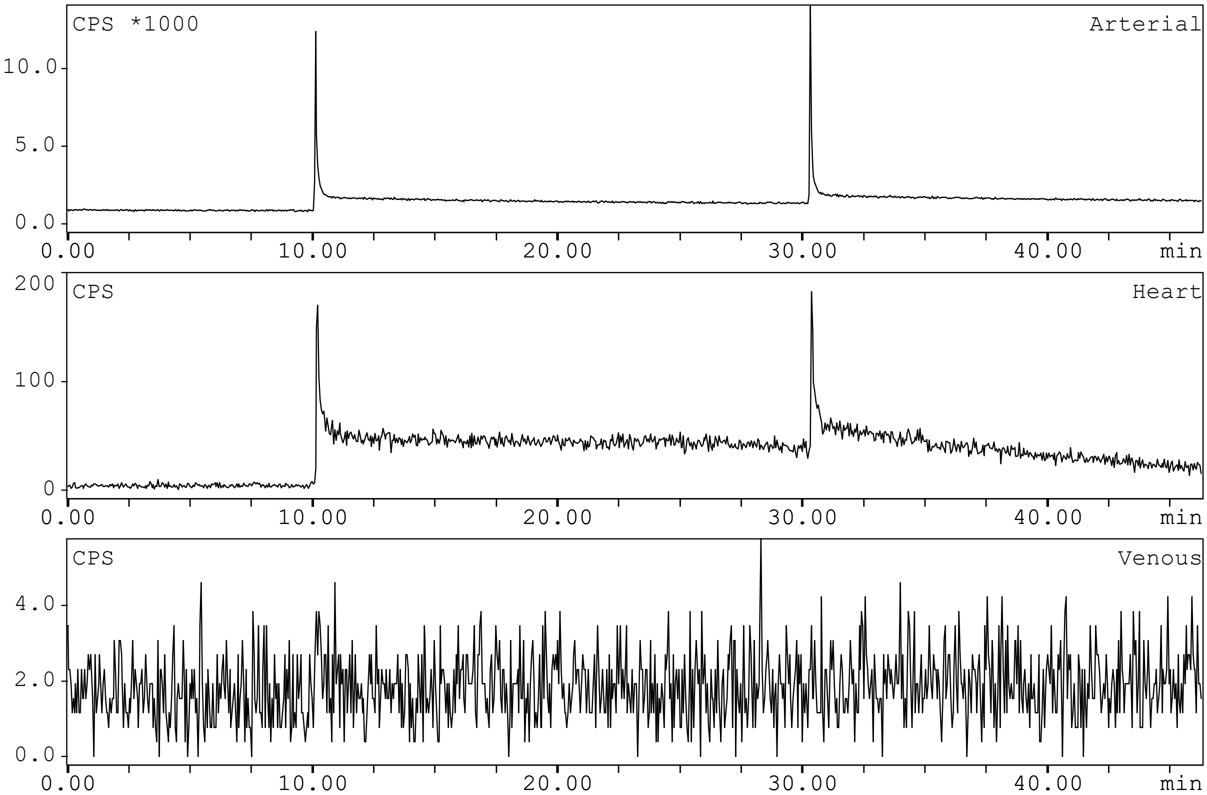

Figure S46: Experiment 3.

Triple γ-Detector System Raw Data for [^{68}Ga]Ga-NODAGA-xy-TXP (**[^{68}Ga]Ga4c**)

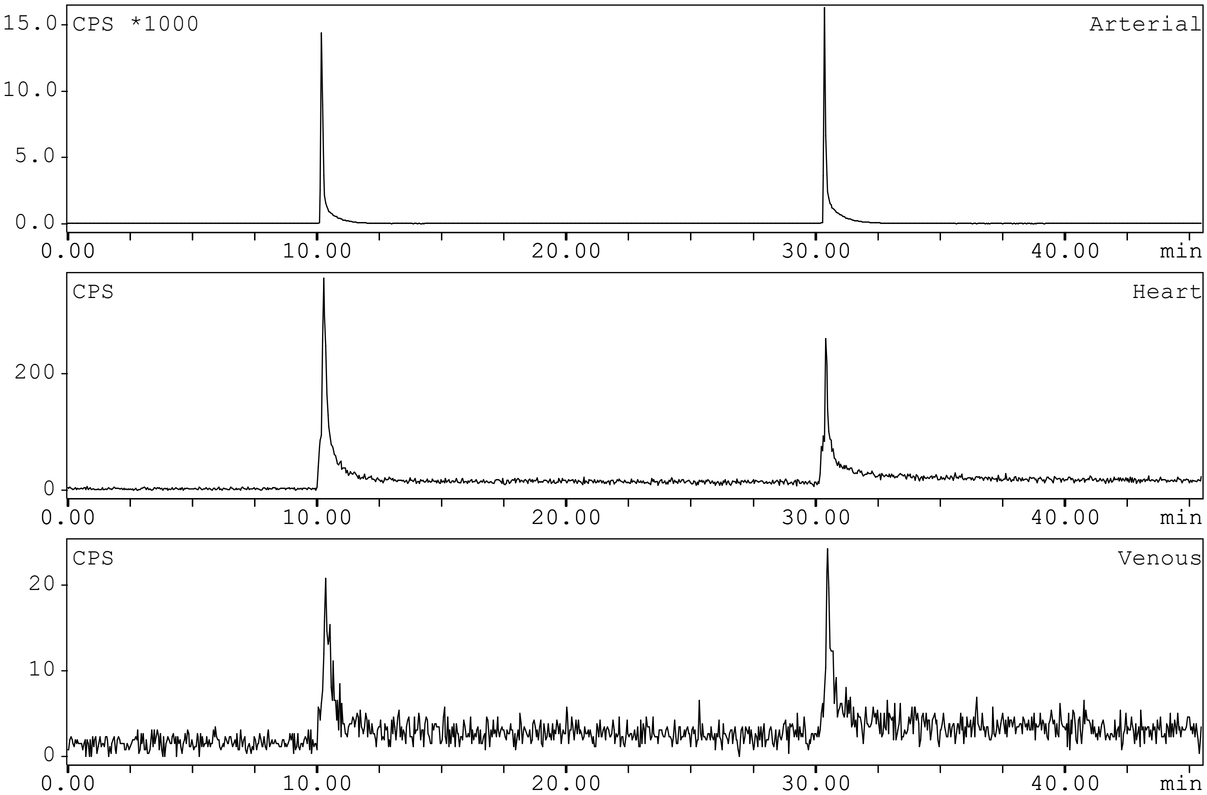

Figure S47: Experiment 1.

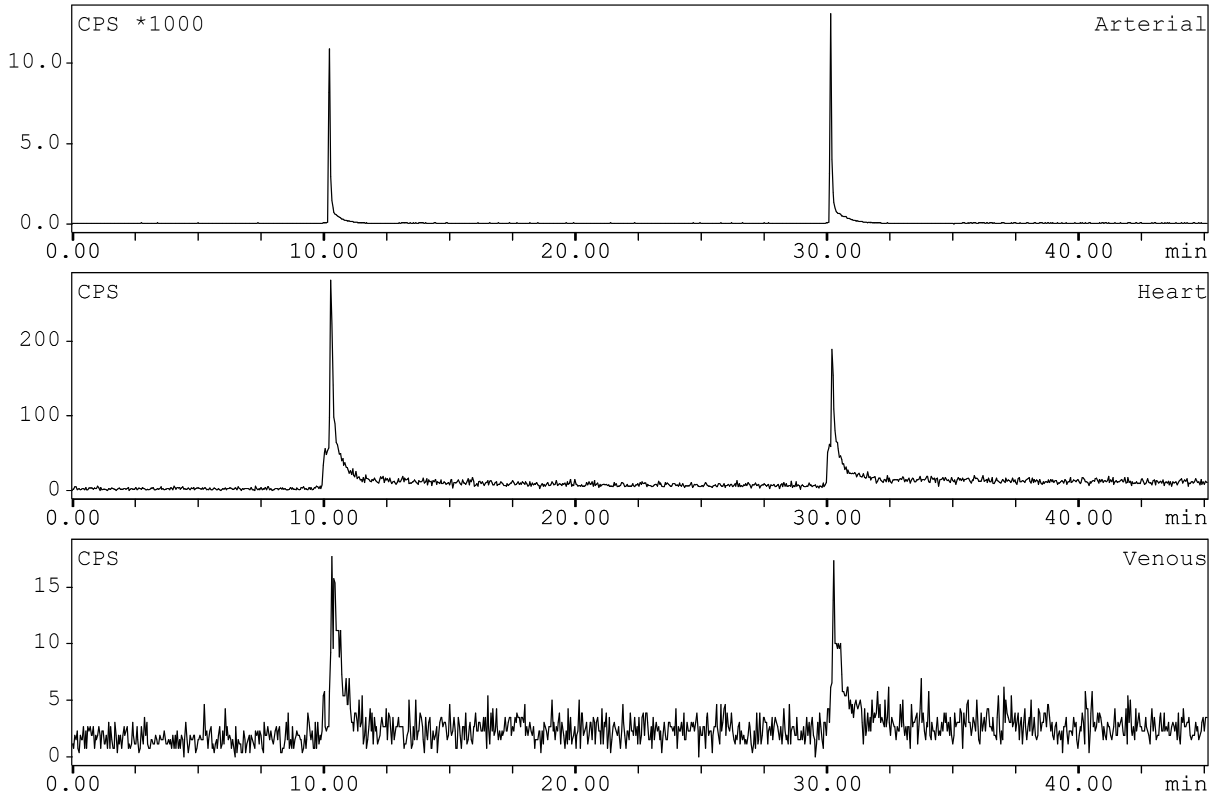

Figure S48: Experiment 2.

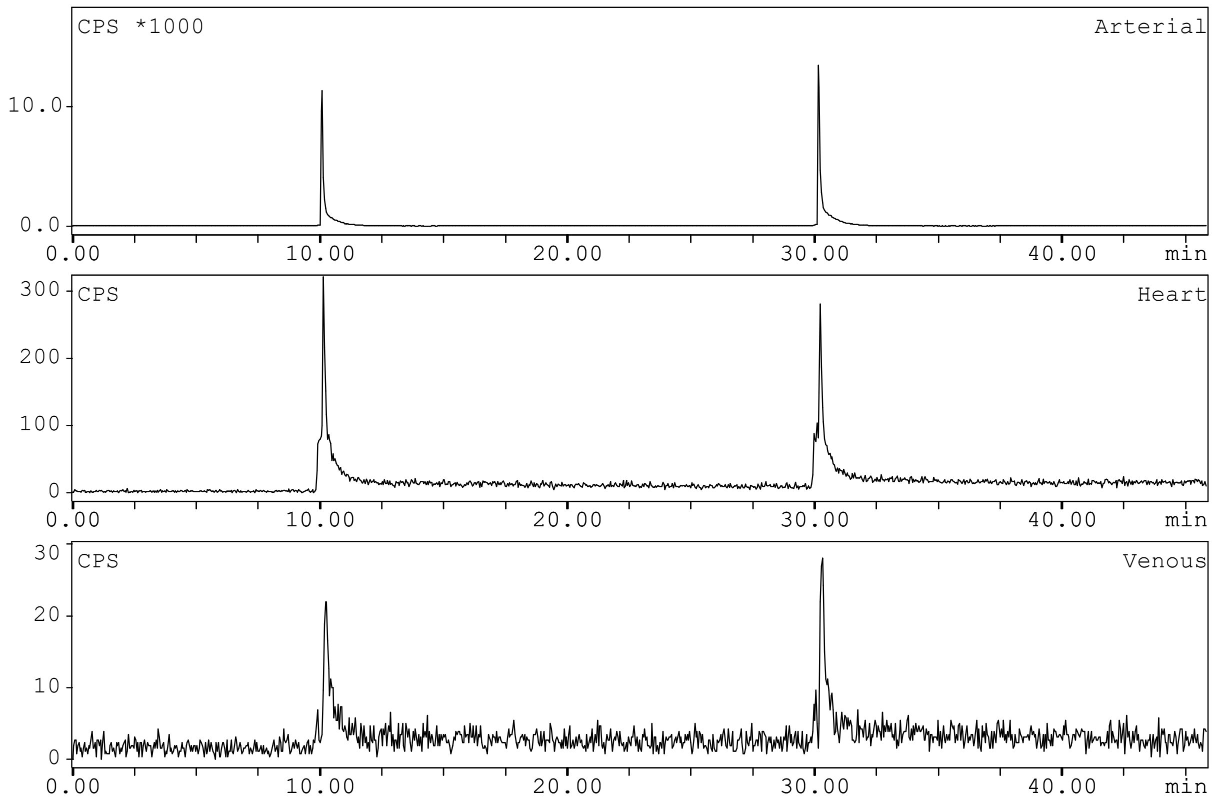

Figure S49: Experiment 3.

DFT Calculations

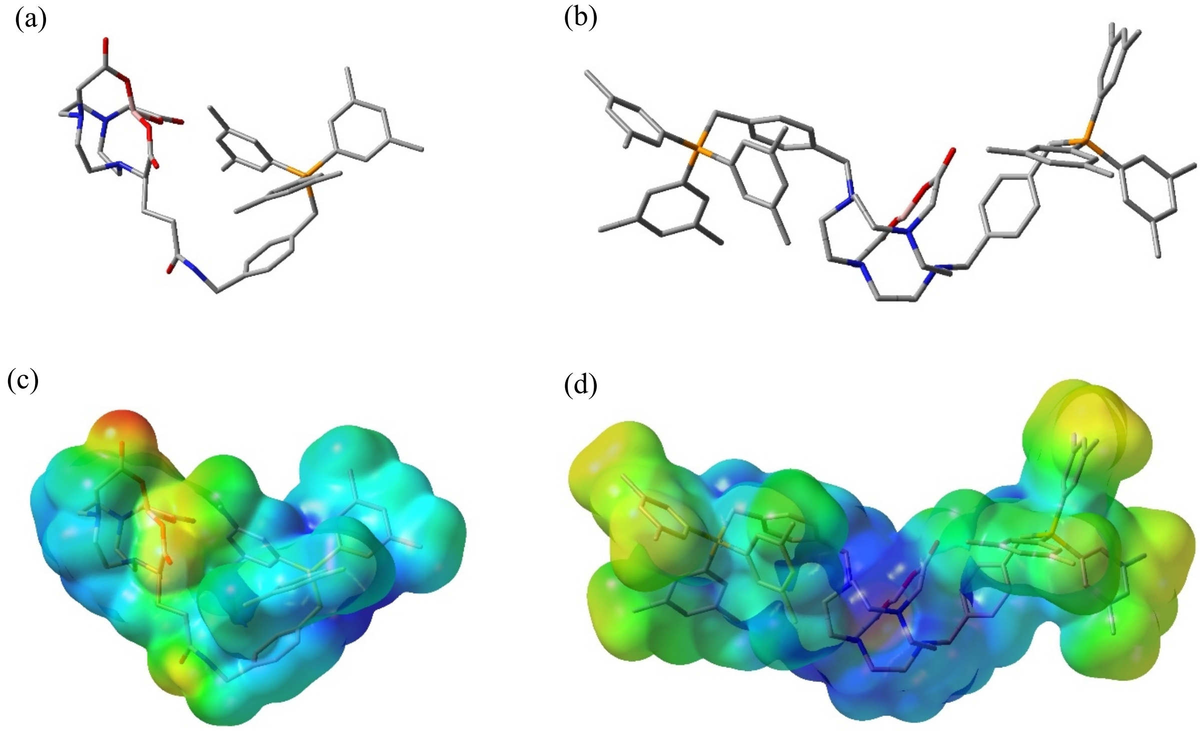

Figure S50: DFT optimised structures of (a) **[Ga(NODAGA-xy-TXP)]$^{+}$** and (b) **[Ga(DO2A(-xy-TXP)$_2$)]$^{3+}$** with a hexacoordinated metal centre (Ga^{3+}). Mapping of the electrostatic potentials of (c) **[Ga(NODAGA-xy-TXP)]$^{+}$** and (d) **[Ga(DO2A(-xy-TXP)$_2$)]$^{3+}$** onto electron density surface; the MEP of (c) represents a maximum potential of 0.12 a.u. and minimum of -0.03 a.u. while the MEP of (d) represent a maximum potential of 0.25 a.u. and minimum of 0.10 a.u. (red to blue = negative to positive).